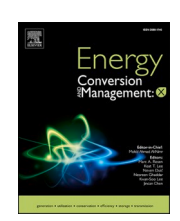
FISEVIER

Contents lists available at ScienceDirect

Energy Conversion and Management: X

journal homepage: www.sciencedirect.com/journal/energy-conversion-and-management-x





Enhancing peak performance forecasting in steam power plants through innovative AI-driven exergy-energy analysis

Muhammad Ali Ijaz Malik ^a, Adeel Ikram ^{a,b,*} , Sadaf Zeeshan ^c, Muhammad Naqvi ^d, Syed Qasim Raza Zahidi ^a, Fayaz Hussain ^{e,f}, Hayati Yassin ^{f,*}, Atika Qazi ^g

- a Smart Manufacturing and Renewable Technologies Laboratory (SMART-Lab), Department of Mechanical Engineering, Superior University, Lahore, Pakistan
- ^b Faculty of Engineering, Chungnam National University, Daejeon 34134, Republic of Korea
- ^c Department of Mechanical Engineering, University of Central Punjab, Lahore, Pakistan
- ^d College of Engineering and Technology, American University of the Middle East, Kuwait
- ^e Department of Biological and Agricultural Engineering, Faculty of Engineering, Universiti Putra Malaysia, Selangor, Malaysia
- f Faculty of Integrated Technologies, Universiti Brunei Darussalam, Brunei Darussalam
- g Centre for Lifelong Learning, Universiti Brunei Darussalam, Brunei Darussalam

ARTICLE INFO

Keywords: Performance optimization Energy-exergy analysis Artificial Intelligence Plant analysis Rankine cycle

ABSTRACT

This study aims to investigate and predict the performance of a 400 MW steam power plant operating on the Rankine cycle through a combined exergy-energy analysis and an artificial intelligence-based random forest regression model. The primary objective is to assess component-wise inefficiencies, identify key parameters influencing plant performance, and develop an optimized predictive model for performance evaluation. A mathematical formulation of energy and exergy balance equations is developed for each plant component and analyzed using the Engineering Equation Solver (EES). The study investigates temperature and pressure gradients, as well as mass flow rates, across all integral components. A parametric analysis is conducted to evaluate the impact of operational parameters on cycle efficiency, exergy destruction, and exergy losses. The results indicate that the boiler experiences significant temperature and pressure gradients, leading to higher irreversibility, whereas the gland steam condenser exhibits lower gradients, resulting in reduced exergy destruction. Among the plant components, the intermediate pressure turbine demonstrates the highest exergetic efficiency (90-93 %), while the condensate extraction pump has the lowest (20-26 %). Similarly, energy efficiency is highest in the intermediate pressure turbine (90-92 %) and lowest in the condensate extraction pump (18-22 %). The study further reveals that steam quality and reheat pressure at the low-pressure turbine outlet significantly influence overall power output and plant efficiency. The mass flow rates of steam through the high, intermediate, and low-pressure turbines follow a ratio of 110:124.3:143.6, with corresponding pressure ratios of 20:2.1:0.071. To enhance predictive accuracy, a random forest regression model is employed to forecast various performance indicators of the steam power plant. The model utilizes 100 decision trees with a maximum depth of 10, enabled bootstrapping, a fixed random seed of 42, and a minimum sample split of 2. The model's predictions for energy and exergy efficiencies are validated against experimental data, with root mean square error (RMSE) and coefficient of determination (R2) computed for accuracy evaluation. The study highlights that the random forest regression model can be utilized to predict and optimize the performance of steam power plants, thereby enhancing their efficiency and minimizing exergy losses.

1. Introduction

Steam power plants in many countries require extensive retrofitting

https://doi.org/10.1016/j.ecmx.2025.101025

^{*} Corresponding authors at: Smart Manufacturing and Renewable Technologies Laboratory (SMART-Lab), Department of Mechanical Engineering, Superior University, Lahore, Pakistan (A.Ikram); Faculty of Integrated Technologies, Universiti Brunei Darussalam, Brunei Darussalam (H. Yassin)

E-mail addresses: aliiijaz@yahoo.com, muhammadali.ijaz@superior.edu.pk (M.A. Ijaz Malik), adeel.ikram@superior.edu.pk, dr.adeelikram@gmail.com (A. Ikram), sadaf.zeeshan@ucp.edu.pk (S. Zeeshan), sayed.naqvi@aum.edu.kw (M. Naqvi), fayazhussain@upm.edu.my (F. Hussain), hayati.yassin@ubd.edu.bn (H. Yassin).

AI Artificial Intelligence I Exergy Destruction ANN Artificial Neural Network J/kgK Joule Per Kilogram Kelvin BFWP Boiler Feed Water Heater K Kelvin CCPPS Combine Cycle Power Plants KW Kilo-watt CCPPS Combine Cycle Power Plants KW Kilo-watt CPEC China-Pakistan Economic Corridor kg/s Kilogram per Second BFP Boiler Feed Pump kJ/kg Kilojoule per Kilogram CEP Condensate Extraction Pump LPT Low Pressure Turbine CEP Condensate Water Supply LNG Liquified Natural Gas CWR Condensate Water Supply LNG Liquified Natural Gas CWR Condensate Water Return MAPE Mean Absolute Percentage Error CC Combustion Chamber MMBH Metric Million Tonnes per Annum CP Condensate Water Pump mtpa Million Tonnes per Annum CP Condensate Water Pump MW Mega-watt Cp Specific Heat Capacity m Mass Flow Rate EES Engineering Equation Solver NTDC National Transmission and Dispatch Company EGT Exhaust gas temperature FWP Feed Water Pump PSO Particle Swarm Optimization GBMs Gradient Boosting Machines GGS Gland Steam Condenser GGC Gland Steam Condenser GGC Gland Steam Condenser GFH Gas Furbine GSC Gland Steam Condenser GFH Gas Furbine HPT High Pressure Turbine HPT High Pressure Turbine HPT High Pressure Turbine HPT High Pressure Generators USD United States Dollar HPT High Pressure Hurbine HPT High Pressure W W Work HIH Heat Losses X Exergy	Nomenc	lature	h	Enthalpy
ANN Artificial Neural Network J/kgK Joule per Kilogram Kelvin BFWP Boiler Feed Water Heater K Kelvin CCPPS Combine Cycle Power Plants kW Kilo-watt CPEC China-Pakistan Economic Corridor kg/s Kilogram per Second BFP Boiler Feed Pump kJ/kg Kilojoule per Kilogram CEP Condensate Extraction Pump LPT Low Pressure CRH Cold Reheat LP Low Pressure Turbine CWS Condensate Water Supply LNG Liquified Natural Gas CWR Condensate Water Return MAPE Mean Absolute Percentage Error CC Combustion Chamber MMBtu Metric Million British Thermal Unit CWP Condensate Water Pump mtpa Million Tonnes per Annum CP Condensate Pump MW Mega-watt CP Specific Heat Capacity m Mass Flow Rate EES Engineering Equation Solver NTDC National Transmission and Dispatch Company EGT Exhaust gas temperature η1 Energy Efficiency FWP Feed Water Pump			IPT	Intermediate Pressure Turbine
BFWP Boiler Feed Water Heater CCPPs Combine Cycle Power Plants kW Kilo-watt CPEC China-Pakistan Economic Corridor BFP Boiler Feed Pump CEP Condensate Extraction Pump CEP Condensate Extraction Pump CRH Cold Reheat LP Low Pressure CWS Condensate Water Supply CWR Condensate Water Return CC Combustion Chamber CC Combustion Chamber MMBtu Metric Million British Thermal Unit CWP Condensate Water Pump MW Mega-watt CCp Specific Heat Capacity ES Engineering Equation Solver FWP Feed Water Pump MTD National Transmission and Dispatch Company EGT Exhaust gas temperature FWP Feed Water Pump BOBMS Gradient Boosting Machines GSC Gland Steam Condenser RMSE Root Mean Square Error GSC Gland Steam Condenser RPR Random Forest Regression h Enthalpy HTT High Pressure Turbine HRSGS Heat Recovery Steam Generators W Work Kelvin KK Kelvin KW Kilo-watt Kilo-watt Kilo-watt KI Kilo-watt MAPE Mean Absolute Percentage Error MBBu Metric Million British Thermal Unit Mass Flow Rate Name Associate Water Pump My Mega-watt Name Associate Water Pump My Mega-watt Name Associate Water Manum Mape Million British Thermal Unit Mass Flow Rate Name Associate Water Million British Kiloman Associate Water Manum Mape Million British Mape Million British Metric Million British Metric Million British Metric Million British Mape Million British Mape Million British Metric Million British Mape Million British Metric Million Mape Million Mape Million Mape M	AI	Artificial Intelligence	I	Exergy Destruction
BFWP Boiler Feed Water Heater CCPPs Combine Cycle Power Plants KW Kilo-watt CPEC China-Pakistan Economic Corridor BFP Boiler Feed Pump CEP Condensate Extraction Pump CFP Condensate Extraction Pump CFP Condensate Extraction Pump CFP Condensate Water Supply CWS Condensate Water Supply CWS Condensate Water Return CCC Combustion Chamber CCC Combustion Chamber CCC Combustion Chamber CCC Condensate Water Pump CP Condensate Water Pump MW Mega-watt CCP Specific Heat Capacity EES Engineering Equation Solver EFWP Feed Water Pump MTD National Transmission and Dispatch Company EGT Exhaust gas temperature FWP Feed Water Pump BOBMS Gradient Boosting Machines GGSC Gland Steam Condenser RAMSE Root Mean Square Error GSC Gland Steam Condenser RAMSE Root Mean Square Error GFH Gas Fuel Heater RAMSE Root Mean Square Error GSC Gland Steam Condenser RAFR Random Forest Regression h Enthalpy HTD High Pressure Turbine HRSGS Heat Recovery Steam Generators W Work Kilo-watt Kilogram per Second KW Kilowatt Kilogram per Second KW Kilowatt Kilogram per Second KW Kilowatt Kilogram per Second Ky Kilogram per Second Kylogliouhe per Kilogram Kilogiouhe per Kilogram LyT Low Pressure W Work	ANN	Artificial Neural Network	J/kgK	Joule per Kilogram Kelvin
CPEC China-Pakistan Economic Corridor BFP Boiler Feed Pump CEP Condensate Extraction Pump LPT Low Pressure Turbine CRH Cold Reheat LP Low Pressure CWS Condensate Water Supply LNG Liquified Natural Gas CWR Condensate Water Return MAPE Mean Absolute Percentage Error CC Combustion Chamber MMBtu Metric Million British Thermal Unit CWP Condensate Water Pump MW Mega-watt CP Condensate Pump MW Mega-watt CP, Specific Heat Capacity MM Mass Flow Rate EES Engineering Equation Solver ET Exhaust gas temperature FWP Feed Water Pump PSO Particle Swarm Optimization GBMs Gradient Boosting Machines GT Gas Turbine GT Gas Turbine GSC Gland Steam Condenser RFR Random Forest Regression h Enthalpy HPT High Pressure Turbine HRSGS Heat Recovery Steam Generators Wallon Dunied States Dollar HP High Pressure W W Work	BFWP	Boiler Feed Water Heater		Kelvin
BFP Boiler Feed Pump	CCPPs	Combine Cycle Power Plants	kW	Kilo-watt
CEPCondensate Extraction PumpLPTLow Pressure TurbineCRHCold ReheatLPLow PressureCWSCondensate Water SupplyLNGLiquified Natural GasCWRCondensate Water ReturnMAPEMean Absolute Percentage ErrorCCCombustion ChamberMMBtuMetric Million British Thermal UnitCWPCondensate Water PumpmtpaMillion Tonnes per AnnumCPCondensate PumpMWMega-wattCPSpecific Heat CapacitymMass Flow RateEESEngineering Equation SolverNTDCNational Transmission and Dispatch CompanyEGTExhaust gas temperatureη1Energy EfficiencyFWPFeed Water Pumpη2Exergy EfficiencyFPFeed PumpPSOParticle Swarm OptimizationGBMsGradient Boosting MachinesQinHeat Energy InputGTGas TurbineRMSERoot Mean Square ErrorGSCGland Steam CondenserR²Coefficient of DeterminationGFHGas Fuel HeaterRFRRandom Forest RegressionhEnthalpysEntropyHPTHigh Pressure TurbineSVMSupport Vector MachineHRHHigh ReheatTTemperatureHPSGsHeat Recovery Steam GeneratorsUSDUnited States DollarHPHigh PressureWWork	CPEC	China-Pakistan Economic Corridor	kg/s	Kilogram per Second
CRH Cold Reheat LP Low Pressure CWS Condensate Water Supply LNG Liquified Natural Gas CWR Condensate Water Return MAPE Mean Absolute Percentage Error CC Combustion Chamber MMBtu Metric Million British Thermal Unit CWP Condensate Water Pump mtpa Million Tonnes per Annum CP Condensate Pump MW Mega-watt Cp Specific Heat Capacity m Mass Flow Rate EES Engineering Equation Solver NTDC National Transmission and Dispatch Company EGT Exhaust gas temperature npa Pso Particle Swarm Optimization GBMs Gradient Boosting Machines Qin Heat Energy Input GT Gas Turbine RMSE Root Mean Square Error GSC Gland Steam Condenser R ² Coefficient of Determination GFH Gas Fuel Heater RFR Random Forest Regression h Enthalpy s Entropy HPT High Pressure Turbine SVM Support Vector Machine HRSGs Heat Recovery Steam Generators USD United States Dollar HP High Pressure	BFP	Boiler Feed Pump	kJ/kg	Kilojoule per Kilogram
CWS Condensate Water Supply CWR Condensate Water Return CC Combustion Chamber CWP Condensate Water Pump CP Condensate Pump MW Mega-watt CP Condensate Pump MY Mass Flow Rate EES Engineering Equation Solver EFO National Transmission and Dispatch Company EFO National Transmission and Dispatch Company EFO Peed Water Pump PSO Particle Swarm Optimization CP FWP Feed Pump PSO Particle Swarm Optimization CP GBMS Gradient Boosting Machines CP Qin Heat Energy Input CP Coefficient of Determination CP GAS Turbine CP Coefficient of Determination CP GAS Fuel Heater CP Coefficient of Determination CP GAS Fuel Heater CP Coefficient of Determination CP COEfficient of Determi	CEP	Condensate Extraction Pump	LPT	Low Pressure Turbine
CWRCondensate Water ReturnMAPEMean Absolute Percentage ErrorCCCombustion ChamberMMBtuMetric Million British Thermal UnitCWPCondensate Water PumpmtpaMillion Tonnes per AnnumCPCondensate PumpMWMega-wattCpSpecific Heat CapacitymMass Flow RateEESEngineering Equation SolverNTDCNational Transmission and Dispatch CompanyEGTExhaust gas temperatureη1Energy EfficiencyFWPFeed Water PumpPSOParticle Swarm OptimizationGBMsGradient Boosting MachinesQinHeat Energy InputGTGas TurbineRMSERoot Mean Square ErrorGSCGland Steam CondenserR²Coefficient of DeterminationGFHGas Fuel HeaterRFRRandom Forest RegressionhEnthalpysEntropyHPTHigh Pressure TurbineSVMSupport Vector MachineHRHHigh ReheatTTemperatureHRSGsHeat Recovery Steam GeneratorsUSDUnited States DollarHPHigh PressureWWork	CRH	Cold Reheat	LP	Low Pressure
CCCombustion ChamberMMBtuMetric Million British Thermal UnitCWPCondensate Water PumpmtpaMillion Tonnes per AnnumCPCondensate PumpMWMega-wattCpSpecific Heat CapacitymMass Flow RateEESEngineering Equation SolverNTDCNational Transmission and Dispatch CompanyEGTExhaust gas temperatureη1Energy EfficiencyFWPFeed Water Pumpη2Exergy EfficiencyFPFeed PumpPSOParticle Swarm OptimizationGBMsGradient Boosting MachinesQinHeat Energy InputGTGas TurbineRMSERoot Mean Square ErrorGSCGland Steam CondenserR²Coefficient of DeterminationGFHGas Fuel HeaterRFRRandom Forest RegressionhEnthalpysEntropyHPTHigh Pressure TurbineSVMSupport Vector MachineHRHHigh ReheatTTemperatureHRSGsHeat Recovery Steam GeneratorsUSDUnited States DollarHPHigh PressureWWork	CWS	Condensate Water Supply	LNG	Liquified Natural Gas
CWP Condensate Water Pump mtpa Million Tonnes per Annum CP Condensate Pump MW Mega-watt Cp Specific Heat Capacity m Mass Flow Rate EES Engineering Equation Solver NTDC National Transmission and Dispatch Company EGT Exhaust gas temperature ntlease per Exhaust gas per Exhaust	CWR	Condensate Water Return	MAPE	Mean Absolute Percentage Error
CPCondensate PumpMWMega-watt C_p Specific Heat CapacitymMass Flow RateEESEngineering Equation SolverNTDCNational Transmission and Dispatch CompanyEGTExhaust gas temperature η_1 Energy EfficiencyFWPFeed Water Pump η_2 Exergy EfficiencyFPFeed PumpPSOParticle Swarm OptimizationGBMsGradient Boosting MachinesQinHeat Energy InputGTGas TurbineRMSERoot Mean Square ErrorGSCGland Steam Condenser R^2 Coefficient of DeterminationGFHGas Fuel HeaterRFRRandom Forest RegressionhEnthalpysEntropyHPTHigh Pressure TurbineSVMSupport Vector MachineHRHHigh ReheatTTemperatureHRSGsHeat Recovery Steam GeneratorsUSDUnited States DollarHPHigh PressureWWork	CC	Combustion Chamber	MMBtu	Metric Million British Thermal Unit
$ \begin{array}{cccccccccccccccccccccccccccccccccccc$	CWP	Condensate Water Pump	mtpa	Million Tonnes per Annum
EESEngineering Equation SolverNTDCNational Transmission and Dispatch CompanyEGTExhaust gas temperature η_1 Energy EfficiencyFWPFeed Water Pump η_2 Exergy EfficiencyFPFeed PumpPSOParticle Swarm OptimizationGBMsGradient Boosting MachinesQinHeat Energy InputGTGas TurbineRMSERoot Mean Square ErrorGSCGland Steam Condenser \mathbb{R}^2 Coefficient of DeterminationGFHGas Fuel HeaterRFRRandom Forest RegressionhEnthalpysEntropyHPTHigh Pressure TurbineSVMSupport Vector MachineHRHHigh ReheatTTemperatureHRSGsHeat Recovery Steam GeneratorsUSDUnited States DollarHPHigh PressureWWork	CP	Condensate Pump	MW	Mega-watt
EGTExhaust gas temperature η_1 Energy EfficiencyFWPFeed Water Pump η_2 Exergy EfficiencyFPFeed PumpPSOParticle Swarm OptimizationGBMsGradient Boosting MachinesQinHeat Energy InputGTGas TurbineRMSERoot Mean Square ErrorGSCGland Steam Condenser \mathbb{R}^2 Coefficient of DeterminationGFHGas Fuel HeaterRFRRandom Forest RegressionhEnthalpysEntropyHPTHigh Pressure TurbineSVMSupport Vector MachineHRHHigh ReheatTTemperatureHRSGsHeat Recovery Steam GeneratorsUSDUnited States DollarHPHigh PressureWWork	C_p	Specific Heat Capacity	ṁ	Mass Flow Rate
FWP Feed Water Pump η_2 Exergy Efficiency FP Feed Pump PSO Particle Swarm Optimization GBMs Gradient Boosting Machines Qin Heat Energy Input GT Gas Turbine RMSE Root Mean Square Error GSC Gland Steam Condenser R ² Coefficient of Determination GFH Gas Fuel Heater RFR Random Forest Regression h Enthalpy s Entropy HPT High Pressure Turbine SVM Support Vector Machine HRH High Reheat T Temperature HRSGs Heat Recovery Steam Generators USD United States Dollar HP High Pressure	EES	Engineering Equation Solver	NTDC	National Transmission and Dispatch Company
FP Feed Pump PSO Particle Swarm Optimization GBMs Gradient Boosting Machines Qin Heat Energy Input GT Gas Turbine RMSE Root Mean Square Error GSC Gland Steam Condenser R ² Coefficient of Determination GFH Gas Fuel Heater RFR Random Forest Regression h Enthalpy s Entropy HPT High Pressure Turbine SVM Support Vector Machine HRH High Reheat T Temperature HRSGs Heat Recovery Steam Generators USD United States Dollar HP High Pressure	EGT	Exhaust gas temperature	η_1	Energy Efficiency
GBMs Gradient Boosting Machines Qin Heat Energy Input GT Gas Turbine RMSE Root Mean Square Error GSC Gland Steam Condenser R ² Coefficient of Determination GFH Gas Fuel Heater RFR Random Forest Regression h Enthalpy s Entropy HPT High Pressure Turbine SVM Support Vector Machine HRH High Reheat T Temperature HRSGs Heat Recovery Steam Generators USD United States Dollar HP High Pressure	FWP	Feed Water Pump	η_2	Exergy Efficiency
GT Gas Turbine RMSE Root Mean Square Error GSC Gland Steam Condenser R ² Coefficient of Determination GFH Gas Fuel Heater RFR Random Forest Regression h Enthalpy s Entropy HPT High Pressure Turbine SVM Support Vector Machine HRH High Reheat T Temperature HRSGs Heat Recovery Steam Generators USD United States Dollar HP High Pressure	FP	Feed Pump	PSO	Particle Swarm Optimization
GSC Gland Steam Condenser GFH Gas Fuel Heater RFR Random Forest Regression h Enthalpy S Entropy HPT High Pressure Turbine HRH High Reheat HRSGs Heat Recovery Steam Generators HP High Pressure W Work	GBMs	Gradient Boosting Machines	Qin	Heat Energy Input
GFH Gas Fuel Heater RFR Random Forest Regression h Enthalpy s Entropy HPT High Pressure Turbine SVM Support Vector Machine HRH High Reheat T Temperature HRSGs Heat Recovery Steam Generators USD United States Dollar HP High Pressure W Work	GT	Gas Turbine		Root Mean Square Error
h Enthalpy s Entropy HPT High Pressure Turbine SVM Support Vector Machine HRH High Reheat T Temperature HRSGs Heat Recovery Steam Generators USD United States Dollar HP High Pressure W Work	GSC	Gland Steam Condenser	R^2	Coefficient of Determination
HPT High Pressure Turbine SVM Support Vector Machine HRH High Reheat T Temperature HRSGs Heat Recovery Steam Generators USD United States Dollar HP High Pressure W Work	GFH	Gas Fuel Heater	RFR	Random Forest Regression
HRH High Reheat T Temperature HRSGs Heat Recovery Steam Generators USD United States Dollar HP High Pressure W Work	h	Enthalpy	S	Entropy
HRSGs Heat Recovery Steam Generators USD United States Dollar HP High Pressure W Work	HPT	High Pressure Turbine	SVM	Support Vector Machine
HP High Pressure W Work	HRH	High Reheat	T	Temperature
	HRSGs	Heat Recovery Steam Generators	USD	United States Dollar
Hl Heat Losses X Exergy	HP	High Pressure	W	Work
	Hl	Heat Losses	X	Exergy

due to low efficiencies and high operational costs [1,2]. However, their relatively low initial capital costs, short commissioning times, and fuel flexibility make them more suitable for developing countries facing budget constraints. Globally, approximately 80 % of power generation comes from fossil fuel sources, while only 20 % is derived from renewable energy sources [3]. The power generation shortfall in developing countries is substantial, e.g., in Pakistan, the power shortfall in 2011 and 2012 was 5000 MW and 6000 MW, respectively. The situation became worse in 2015 with the power generation shortfall reaching 7000 MW [4,5]. In 2014, the Pakistani government, in collaboration with the Chinese government, took serious initiatives to get rid of the energy shortfall. The China-Pakistan Economic Corridor (CPEC) secured a\$34 billion investment for power projects in Pakistan. These projects are expected to contribute over 17,000 MW to the national grid, fulfilling approximately 80 % of the country's energy demand, according to the National Transmission and Dispatch Company (NTDC) [6]. The rising cost of petroleum fuels has led to a shift toward operating power plants with lower-cost fuel alternatives. The accessibility of liquified natural gas (LNG) in Pakistan because of subsidized imports from Qatar, is the prime justification for its utilization in steam power plants. In 2013-14, the primary energy mix entailed 44 % of energy requirements fulfilled by natural gas, and out of 44 %, 27.5 % of total natural gas was utilized in the power sector. In 2019, the LNG comprised 61.7 % of the power generation mix of Pakistan, followed by 27.3 % hydel sources, 15.9 % coal, and 13.5 % oil [7]. The government first imported LNG in 2015 from Qatar to increase reliance on LNG and decrease reliance on other petroleum sources. In the financial year 2021–22, a total of 373 MMBtu of LNG was imported at \$3.4 billion [8]. In 2023, Pakistan's LNG import capacity is projected to increase from 17.1 mtpa in 2023 to 31.7 mtpa in 2030 [9]. The thermal power plants' performance was traditionally assessed using energy analysis, primarily based on the first law of thermodynamics. However, recently, exergy

analysis, rooted in the second law of thermodynamics, has emerged as a more comprehensive approach for evaluating and optimizing power plant performance [10,11]. Exergy analysis goes beyond energy analysis by not only identifying the root causes of irreversibility within the plant but also by evaluating the efficiency of individual components and quantifying the extent of heat losses. This analysis provides a clear picture of the system's state relative to equilibrium and offers insights into effective natural resource conservation strategies. Irreversibility, often referred to as exergy destruction, represents the disparity between the actual useful work generated and the theoretically reversible work—an essential focus of exergy analysis. Furthermore, exergy analysis differentiates between internal process irreversibility, energy losses to the environment, and the quality of energy lost during real-world operations [12,13].

Exergy is comprised of four components, with two main components (physical and chemical). The chemical exergy is linked with the deviation of the system's chemical composition from the equilibrium state, while the physical exergy represents the maximum theoretical useful work achieved by the system during its interaction with the equilibrium state [14]. Excessive energy (heat) is required in the case of highpressure components (evaporator) to change the saturation liquid state of feedwater to the saturation vapor state, which leads to a higher temperature drop of flue gases and ultimately leads to higher exergy destruction. However, lower energy (heat) is required in the case of intermediate/lower pressure components to superheat the vapors, as the economizer already preheats the feedwater. Steam quality plays a critical role in exergy destruction. The lowering of steam quality below saturation leads to higher gross power of the steam turbine as the potential for work significantly increases, but moisture content increases, which results in corrosion of the turbine blade and reduces the turbine's life. Moreover, the exergy destruction rate increases, which ultimately results in lower exergy efficiency. The exergy destruction rate in a

condenser increases with steam quality as the temperature of the cooling water increases due to a higher heat transfer rate. Elhelw et al. [15] found an exergy destruction rate in the case where the boiler is at the top (75%), trailed by the turbine (15%) and the condenser (6%). Increasing the temperature of both IPT and HPT by 45 °C resulted in power savings of 15.6 % at half load and 17.7 % at full load. The turbine power is inversely proportional to superheat/reheat pressure, but the turbine's life is compromised for lower superheat/reheat pressure beyond the critical value. Aliyu et al. [16] found that the increase in cooling water temperature beyond the required limit resulted in improper condensation and threatened aquatic life and environmental protocol, i.e., the cooling water is expelled to sea at a temperature 1 $^{\circ}\text{C}$ higher than the designated temperature if the cooling water flow rate decreased by 15 %. Kaska et al. [17] found energy/exergy efficiencies of the system were 10.2 %/48.5 % and 8.8 %/42.2 %, respectively, for two distinct conditions. Aljundi [18] found energy losses of 134 MW in the condenser, and 13 MW of energy in the boiler was noted. The exergy loss ratio in the boiler (77 %), turbine (13 %), and condenser (9 %) was computed. Exergy efficiency of 25 % and energy efficiency of 26 % were achieved. Vosoogh[19] concluded that the energy and exergy efficiency increased by 0.19 and 0.37 % by decreasing combustion excess air from 0.4 to 0.15. Moreover, with the decline in the temperature of smoke from 137 to 90 °C, the energy and exergy efficiency were increased by 0.84 and 2.3 %, respectively. Regulagadda et al. [20] reported a total exergy destruction of 84,193 kW and a total heat loss of 50,456.5 kW. The highest exergy destruction of 73,046 kW in the boiler and the lowest exergy destruction of 375 kW in the feed pump were noted. The boiler generated maximum entropy of 3312 kW/K and the boiler feed pump generated the least entropy of 0.03 kW/K. The factors, like throttling in valves, heat loss, and steam leakage, contribute to exergy loss.

Kaushik et al. [21] concluded that the highest energy loss occurred in the condenser, and the highest exergy loss occurred for the boiler. It can be credited to an incomplete combustion process, incongruous heat insulation, and entropy generation in the device. Pattanayak et al. [13] observed the highest exergy efficiency of 97.34 % and energy efficiency of 95.68 % in the case of an intermediate pressure turbine. The condenser exhibited the lowest exergy efficiency of 29 % and an energy efficiency of 66.36 %. The exergy efficiency in the case of the compressor and HRSG was 93.96 and 87.20 %, respectively. Ameri et al. [22] observed that combustion chambers, gas turbines, duct burners, and heat recovery steam generators are the main sources of irreversibility, entailing 83 % of total exergy loss. In another study, Ameri et al. [23] accounted for maximum energy losses of 306.9 MW from the condenser (81 % of total exergy destruction) and 67.63 MW from the boiler (5 % of total exergy destruction). The maximum irreversibility can be accounted for in the boiler because of the higher temperature associated with the combustion reaction, and it can be decreased by decreasing the air-fuel ratio and preheating the combustion air. Isam Aljundi [18] also concluded that the exergy loss ratio in the boiler can be reduced through air preheating and reducing the fuel-to-air ratio. Ahmadi and Toghraie [24] observed 32 % energy efficiency and 35.2 % exergy efficiency with a total exergy destruction of 368.18 MW. The energy and exergy losses in the condenser were 296.8 MW and 5.63 MW, with an exergy loss ratio of 69.8 and 1.53 %, respectively. The energy and exergy losses in the boiler were 42.9 MW and 315.39 MW, with an exergy loss ratio of 10.16 and 85.66 %, respectively. Rudiyanto et al. [25] found an exergy efficiency of 26.36 %, and this efficiency increased to 94.04 % at 41 bar pressure. They found a direct relation between output pressure, steam input quality, gross power, and efficiency of the turbine. The irreversibility of the boiler, condenser, turbine, LPH, HPH, pump and deaerator were 1677003 kW (17.28 %), 738122 kW (7.61 %), 152894 kW (1.58 %), 111881 kW (1.15 %), 470520 kW (4.85 %), 193494 kW (1.99 %) and 1081771 kW (11.15 %), respectively. Pilankar and Kale [26] revealed through exergy analysis that the highest exergy destruction of 238.6 MW was accounted for by the boiler, which represents 90.8 % of the total exergy destruction of the plant. Exergy

destruction of 4.426 MW was accounted for by the condenser, which represents 1.78~% of total exergy destruction. The total energy and exergy loss for the plant were 89.17~MW and 260.7~MW. It was observed that the energy efficiencies of components were higher than the exergy efficiencies.

Danish et al. [27] explored the transformation of energy models to align with machine learning techniques for optimizing combined cycle power plants (CCPPs). Using the Broyden Fletcher Goldfarb Shanno (BFGS) algorithm, the proposed numerical model improved operational efficiency, increasing power output by 2.23 % from 452 MW to 462.1 MW through optimized environmental factors. The study highlights the potential of AI-based modeling for forecasting and decision-making in complex energy systems. In addition, Assareh et al. [28] proposed a system that integrates a Multi-Effect Distillation (MED) unit with Thermal Vapor Compression (TVC) and dual-pressure heat recovery steam generators. The study aims to reduce costs, lower CO₂ emissions. and improve both power output and energy efficiency through optimization using artificial neural networks and genetic algorithms with EES and MATLAB. The upgraded system boosts energy efficiency by over 10 % and reduces CO2 emissions by 23 %, and improves the exergy efficiency from 31 % to 41 %. Beiron et al. [29] studied the role of combined heat and power (CHP) plant flexibility as a strategy for handling variations while assessing cost-effectiveness. Using an energy system optimization model, the study examines the interaction between electricity and district heating in a Swedish price area, and the results indicate that CHP investments are primarily driven by district heating demand rather than electricity needs, resulting in limited capacity to influence electricity system variations. Moghaddam et al. [30] performed an analysis of variance through a central composite design technique to examine the impact of pressure, temperature, and steam/feed ratio. They achieved optimum values of 900 °C temperature, 4 bar pressure, and 0.675 steam/feed ratio.

Artificial Intelligence (AI) techniques have been extensively employed to predict the performance of steam power plants, offering substantial improvements in operational efficiency and system reliability. These AI-driven models harness historical operational data to identify complex patterns and correlations that may elude conventional analytical approaches. Moreover, machine learning algorithms facilitate adaptive learning, allowing for continuous model refinement and realtime performance monitoring. This dynamic capability enables predictive maintenance, minimizing the risk of equipment failures and unplanned downtime. The integration of Artificial Intelligence methodologies into power plant operations not only optimizes performance but also enhances the sustainability of energy production by improving resource utilization and reducing operational costs. Although various AI models have been employed, including Support Vector Machines (SVM), Artificial Neural Networks (ANN), and Gradient Boosting, but Random Forest regression model is often regarded as a superior choice for predicting the performance of steam power plants. SVMs are adept at handling non-linear relationships and delivering robust classification and regression outcomes; however, they often require extensive training time due to their computational complexity, especially with large datasets. ANNs are highly effective in modeling intricate, nonlinear systems and extracting valuable insights from historical data, yet they also demand significant computational resources, leading to prolonged training durations. Gradient boosting machines (GBMs) enhance predictive accuracy through iterative error reduction, but they are susceptible to overfitting without meticulous tuning. In contrast, the random forest regression model (RFRM) provides distinct advantages through its ensemble learning methodology, which combines multiple decision trees to deliver high accuracy and robustness. This approach not only effectively reduces overfitting but also efficiently manages noisy or imbalanced data, offering reliable predictions and valuable insights into feature importance. These attributes make the RFRM particularly well-suited for complex performance forecasting in steam power plants, Table 1 mentions the advantages and disadvantages of the

Table 1Comparison of commonly used AI methods with Random Forest for power plant performance optimization.

AI Method	Advantages	Disadvantages
Support Vector Machines (SVM)	Effective in handling non- linear relationships [31] Delivers robust outcomes [32]	Computationally intensive, especially with large datasets [33] Requires extensive training time [34]
Artificial Neural Networks (ANN)	Highly effective in modeling complex systems [35] Capable of extracting valuable insights from historical data [32]	Demands significant computational resources [36] Prolonged training durations [37]
Gradient Boosting Machines (GBM)	Enhances predictive accuracy through iterative error reduction [38]	Susceptible to overfitting without meticulous tuning [39] Computationally expensive [40]
Random Forest Regression (RFR)	High accuracy and robustness through ensemble learning [41] Effectively reduces overfitting [42] Manages noisy or imbalanced data well [43]	Random Forest, while accurate, can be more difficult to interpret than simpler models like decision trees [44] Requires careful tuning of parameters to optimize performance [42]

AI models used for optimization of power plant parameters and performance.

Many authors have used artificial intelligence models for predictions of the performance of power plants. Haddadin et al. [45] used an artificial neural network (ANN) model to predict the behavior of variables and power output. Similarly, ANN was used by Park et al. [46] for energy demand and supply matching in PV power generation, with an accuracy of the model being 13.2 %. Moreover, ANN models using metaheuristic optimization algorithms have also been used to predict power plant performance. Moustafa et al. [47] used a humpback whale optimizer to predict energy efficiency and exergy efficiency with a correlation coefficient ranging from 0.98 to 0.99. Also, Esfandyari et al. [48] used ANN along with particle swarm optimization (PSO) to forecast the heat transfer rate, having correlation coefficients of the model being greater than 94.84 %. Furthermore, water desalination using heat recovery of a real thermal power plant was done by Assareh et al. [49] where the ANN model was deployed to compute exergy efficiency, carbon dioxide emission, and net power output. Similarly, Esfandyari et al. [50] also used an adaptive neuro-fuzzy inference system (ANFIS) tuned by a particle swarm optimization (PSO) algorithm to predict sulfur removal from diesel fuel with favorable results. SVM has also been used to optimize various output parameters of power plants. Cai et al. [51] used PSO-SVM classifier for arc-fault detection of solar PV power generation systems. Furthermore, Ashraf et al. [52] used SVM to achieve the efficient power production operation of a 660 MW coal power plant. Moreover, Lin et al. [53] predicted photovoltaic power generation using SVM accurately, whereas Tuerxun et al. [54] used SVM for fault diagnosis of wind turbines. Similarly, Singh et al. [55] used a Gradient Boosting approach to forecast wind production with a mean absolute error (MAE) value of 0.0277, a mean absolute percentage error (MAPE) value of 0.3310, and a root mean square error (RMSE) value of 0.0672. Also, Mitrentsis et al. [56] predicted solar power production accurately using Gradient Boosting.

The application of AI, specifically the RFRM, a relatively underutilized algorithm in power plant analysis, presents a novel approach to energy and exergy evaluation. Random Forest excels in managing large datasets, accurately capturing complex non-linear interactions, and significantly enhancing predictive accuracy. Furthermore, it minimizes overfitting by aggregating predictions from multiple decision trees, thereby reducing variance and improving model generalization. This method provides robust and reliable insights into thermal system

performance, streamlining analytical processes and advancing the precision and depth of system evaluation in power plants. The random forest regression model has been successfully employed to make predictions in several applications. Huang et al. [57] used the random forest regression model to predict carbon peak predictions with an R² of 0.94. Danish et al. [27] explored the transformation of energy models to align with machine learning techniques for optimizing combined cycle power plants (CCPPs). Using the Broyden Fletcher Goldfarb Shanno (BFGS) algorithm, the proposed numerical model improved operational efficiency, increasing power output by 2.23 % from 452 MW to 462.1 MW through optimized environmental factors. The study highlights the potential of AI-based modeling for forecasting and decision-making in complex energy systems. Random forest regression model (RFRM) has been successfully employed to make predictions in several applications. Achmad et al. [58] used RFRM to forecast coal power plant retirement ages, whereas Alexandra et al. [59] predicted solar power generation using the RFRM model. Furthermore, RFRM has been used to predict solar irradiance at high altitudes [60] and at different sunshine hours [61]. A regression model using random forest has also been applied to predict wind power production [62–65] as well as to successfully predict wind turbine noise [66-68]. RFRM has even been used to predict the mechanical properties of substances like aluminum alloys [69], and the compressive strength of basalt fiber [70], as well as to predict air-water interfacial tension in conventional and peptide surface-active agents [71]. RFRM has also found its use in applications like fatigue life prediction of bending polymer films [72] and estimation of moisture in live fuels [73]. Moreover, RFRM has been used for effective prediction and analysis of commercial wood fuel blends used in a typical biomass power station [74] as well as prediction of harbor fuel consumption [14], finding that the meteorological factors collectively add value to fuel consumption prediction and improve its accuracy. RFRM has also successfully been able to optimize biodiesel production by successfully predicting biodiesel yield [75]. In short, the machine learning model using random forest can be successfully used to make accurate predictions in many important applications and hence in turn lead to system optimization and efficiency improvements [76].

The primary objective of this study is to conduct an exergy analysis of the Balloki thermal power plant (a reference thermal power plant and real data are used), which has a unit capacity of 400 MW. The analysis is performed using the Engineering Equation Solver (EES) software [24]. The current study aims to investigate the factors affecting power plant performance to optimize power plant efficiency. However, the innovation lies in artificial intelligence (AI) integration with exergy analysis for power plant performance optimization. The current study investigates the influence of pressure, temperature, and mass flow rate variations across each process component on a power plant's energy and exergy performance. Moreover, it advances an AI approach for optimizing the plant's performance, which improves the accuracy of performance predictions in comparison with conventional methods. To achieve the set objective, the principles of mass, exergy, and energy conservation are applied to each component of the Balloki power plant. Such a comprehensive analysis ascertains the fundamental performance indicators such as exergy efficiency, energy efficiency, relative exergy destruction, exergy loss ratio, and overall plant efficiency. Engineering equation solver (EES) software permits the classification of optimal operational parameters for power plant performance enhancement. The novelty of current research lies in the unique combination of exergy analysis and AI-based optimization to identify inefficiencies and optimize Balloki power plant performance, which has been underexplored in the previous literature. The initial phase of this study involves recognizing the imperative need for efficient energy utilization and establishing clear objectives to attain these goals. Subsequently, exergy analysis is employed to identify the root causes, positions, and magnitudes of process inefficiencies within the system. The empirical approach is then integrated with AI optimization for the improvement in power plant performance. Table 2 presents a comparative analysis of the current

 Table 2

 A comparative analysis of the current study and the literature review.

No	Powerplant name/	Capacity	Energy effic	nergy efficiency (%)					Exergy efficiency (%)				
	country/reference		Boiler	Turbine	Condenser	Pump	Cycle	Boiler	Turbine	Condenser	Pump	Cycle	
•	Eastern Province, Saudi Arabia [77]	1240 MW	-	_	-	-	_	=	92.05	62.98	-	-	
•	Montazeri Steam Power Plant, Iran [78]	200 MW	90.55	78.28(HPT)87.34 (IPT)80.62 (LPT)	_	68.1 (BFP)69 (CWP)	32	44.5	87.67 (HPT) 91.08 (IPT) 82.62 (LPT)	_	90.5 (BFP)83 (CWP)	35.2	
	Yatagan Power Plant, Turkey [79]	630 MW	-	_	-	-	37.01	40.84	80.1	62.72	60.66 (CP) 64 (CP,2)60.85 (FWP)	31.95	
•	412 MW Power Plant [80]	412 MW	96.90 (CC)	88.12 (HPT)95.68 (IPT)86.82 (LPT)	66.36	-	_	77.48 (CC)	93.41 (HPT) 97.34 (IPT) 86.96 (LPT)	29	-	_	
	32 MW coal-fired power plant [81]	32 MW	_	_	_	_	25.38	_	_	_	_	23.17	
5.	Can Powerplant, Turkey [79]	320 MW	_	_	-	_	42.12	48.23	84.85 (HPT) 96.12 (IPT) 90.03 (LPT)	80.22	60.82 (CP)63.99 (CP,2)58.83 (FWP)	37.88	
7.	Neyveli Powerplant [82]	50 MW	91.9	26.91	_	_	_	58.62	81.2	_	_	32.46	
•	Al-Hussein power plant, Jordan [83]	396 MW	_	_	_	_	26	43.8	73.5	26.4	82.5(BFP)	24.8	
	Shenyang CHP Power Station [84]	50 MW	84.89	78.5	_	84.77 (FWP)	_	30.04	49.21	_	63.38(FWP)	-	
0.	Orhaneli, Bursa Province, Turkey [79]	210 MW	_	-	_	-	37.63	45.77	90.51 (HPT) 90.97 (IPT) 64.42 (LPT)	68.98	90.68 (CP)92.42 (CP,2)75.03 (FWP)	35.49	
1.	250 kW Steel Industry Power Plant [85]	250 kW	_	-	_	_	_	76.1 (Case a)72.1 (Case b)	80.0 (Case a) 77.0 (Case b)	44.7 (Case a) 63.8 (Case b)	71.5 (Case a)73.9 (Case b)	48.5 (Case a 42.2 (Case b	
2.	Soma Station [79]	500 MW	-	_	-	-	36.08	41.43	85.12 (HPT) 89.99 (IPT)86 (LPT)	47.33	65.67 (CP) 65.77 (CP,2)70.36 (FWP)	32.35	
3.	MARAFEQ Power Plant, Arab Saudi [86]	2700 MW	61.8 (CC)	82 (GT)	_	92 (Air Compressor)	34.33	68.3 (CC)	91.6 (GT)	-	94.9 (Air Compressor)	32.38	
4.	Kangal [79]	457 MW	-	_	_		37.19	36.45	90.86 (HPT) 92.94 (IPT) 84.19 (LPT)	62.65	41.24 (CP)58.91 (CP,2)60.5 (FWP)	28.55	
5.	Malay Peninsula 396 MW CC Powerplant [87]	396 MW	_	-	_	_	_	41.5	92.7 (HPT) 92.1 (IPT)67.5 (LPT)	90.83	96.31 (Air Compressor)	_	
6.	Kostolac B Power Plant [88]	348.5 MW	_	-	_	_	_	46.4	89.7 (HPT) 91.6 (IPT)79.3 (LPT)	57.8	82.7 (1)85.0 (2)	35.8	
7.	Jawa Power-YTL, Paiton, Indonesia [89]	610 MW	47.98	54.66–84.53	8.94	34.13	_	48.06	93.23–99.92	0.796	33.03	26.36	
18.	Afsin Elbistan [79]	1440 MW	-	_	_	_	42.64	39	94.22 (HPT) 97.89 (IPT) 86.16 (LPT)	59.74	78.73 (CP)78.74 (CP,2)78.51 (FWP)	32.46	

No	Powerplant name/	Capacity	Energy effic	iency (%)				Exergy effici	ency (%)			_
	country/reference		Boiler	Turbine	Condenser	Pump	Cycle	Boiler	Turbine	Condenser	Pump	Cycle
19.	Seyitomer Powerplant [79]	600 MW	-	-	-	-	38.03	36.75	96.75 (HPT) 95.98 (IPT) 85.45 (LPT)	47.33	81.49 (CP)83.29 (CP,2)86.53 (FWP)	31.50
20.	23.8 MW Powerplant [90]	23.8 MW	91.87 (1) 92.58 (2)	93.84 (1)93.19 (2)	-	58.3 (FP,1)61.8 (FP,2)	35.29 (Cycle1) 32.07 (Cycle2)	42.06 (1) 42.28 (2)	73.47 (1) 72.24 (2)	_	33.86 (FP,1)36.29 (FP,2)	66.3 (Cycle1) 64.33 (Cycle2)
21.	Catalagzi Power Plant [79]	300 MW	-	-	-	-	37.88	45.47	90.32 (HPT) 88.93 (IPT) 88.6 (LPT)	54.72	67.37 (CP)66.82 (CP,2)69.78 (FWP)	35.19
22.	South Pars Gas Complex [91]	_	89.59	89.5	86.4	81.5	41.2	40.5	95.78	54.6, 63.9	96.68	33.6
23.	Bokaro thermal power station [92]	210 MW	88.92	77.31,84.6,78.9	44.3	72.9	32.9	44.3	83.2,85.3,81.9	49.3	83.9	34.5
24.	GT Power Plant, Egypt [93]	125 MW	_	_	_	_	28.8	71.2	95.3	_	87.4	27.1

Current Work (Balloki Power Plant in Pakistan-400 MW)

'Con	'Components /Loading conditions		Energy effic	ciency (%)			Exergy efficiency (%)			
			44.5 %	78.75 %	87.80 %	98.80 %	44.5 %	78.75 %	87.80 %	98.80 %
1	Turbine	НРТ	76.75	77.23	79.38	79.99	83.16	86.75	87.63	87.94
		IPT	89.75	89.83	90.94	92.05	90.44	92.79	93.00	93.37
		LPT	68.26	69.34	69.99	72.68	69.27	70.65	71.29	74.19
2	CEP		17.60	20.29	21.43	22.08	19.84	23.86	24.79	25.98
3	GSC		83.58	84.67	89.26	89.36	71.43	72.50	73.64	74.73
4	GFH		55.50	57.00	59.24	69.90	30.99	33.75	37.01	51.05
5	BFWP		22.76	26.62	30.44	30.57	27.59	33.59	33.85	36.47
6	Boiler		85.26	85.92	90.82	91.18	39.11	40.85	42.51	43.05
7	Condenser		69.52	77.57	80.33	95.68	37.73	46.96	50.91	55.95
8	Cycle		26.19	27.90	28.23	30.45	31.33	35.19	35.30	36.04

research findings with the existing literature, highlighting the unique contributions of this study.

2. Methodological framework and data analysis approach

In the current study, the liquefied natural gas (LNG)-fueled Balloki power plant is selected for the exergy analysis. The current study only observed the Rankine process, which is a part of the entire Balloki power plant (the whole power plant is a Combined Cycle Power Plant with a cumulative capacity of 1223 MW). The boiler serves as a Heat Recovery Steam Generator in a combined cycle power plant. The plant is equipped with a 400 MW three-cylinder turbine, including a higher-pressure turbine (HPT), intermediate pressure turbine (IPT), and lower pressure turbine (LPT). The HPT has a total of 30 stages, IPT has 18, and LPT has 10 stages. The chemical composition of fuel is shown in Table 3.

2.1. Plant layout

The schematic diagram of the Rankine cycle power plant is displayed in Fig. 1 (a). The water tube boiler produces steam to run the steam power cycle. Water is pumped through a boiler feed water pump (BFWP), enters the boiler at point 14, and is heated through LNG combustion. The boiler provides dry superheated steam at a designated temperature. The starting section of the boiler, from point 14, possesses a higher temperature compared to the ending portion of the boiler. Therefore, the generated high-pressure steam is sent to high-pressure steam (HPT) as shown in point 1. The low-pressure steam at the end of the boiler is sent to the low-pressure turbine, as shown in point 5. The fuel used for burning is pre-heated in a Gas Fuel Heater (GFH) from the water coming out from the boiler (point 11) to increase the efficiency of the cycle. The remaining water released from GFH at point 12 was reentered into BFWP at point 13. The produced steam then rotates the blades of the steam turbine (ST), which is coupled to a synchronous generator to generate electrical energy. There are 3-cylinder turbines, including High Pressure (HPT), Intermediate Pressure (IPT), and Low Pressure (LPT). HP superheated steam (HP superheater) with 587 °C and 170 bar drives HPT and then returns to HRSG as Cold Reheat (CRH), which passes through the Reheat portion of the boiler (point 2) and is converted into Hot Reheat (HRH) with 587 °C and 35 bar. HRH is now used to drive IPT as shown in point 3. The low-pressure steam from the boiler (point 5) and IPT (point 4) is entered into LPT at point 6. Finally, the LP superheated steam at 273 $^{\circ}\text{C}$ and 4 bar drives the LPT and is then condensed in the turbine. The valves are used to regulate steam pressure for the smooth operation of power plants. The steam from LPT directly comes to the main condenser at point 7. Point 18 shows the cooling water supply to the condenser, and point 19 shows the cooling water return from the condenser. CEP picks condensate water at point 8, and this water is then transferred to GSC at point 9, where it heats up by 1 $^{\circ}$ C. The other side of GSC is linked with a router steam turbine to receive leaked steam, and it is used for heating condensate water, as shown in point 10. The exhaust steam is then allowed to condense through a water

Table 3 Chemical composition of LNG.

Gas Fuel Composition	%
Methane	87.9
Ethane	4.49
Propane	0.35
Iso-Butane	0
N-Butane	0.052
Pentane	0
Iso-Pentane	0.025
Neo-Pentane	0
N_2	5.68
CO_2	2.34
Hexane	0

condenser, which sucks steam at very low pressure and allows steam expansion through the turbine at lower pressure ($-85~\rm kPa$ to $-93~\rm kPa$). The condensate, along with some fresh makeup feed water, is again fed into the boiler by a condensate extraction pump (CEP), which passes through a Gland Steam Condenser (GSC). The technical specifications and details of the steam power plant are displayed in Table 4. The gas cleaning system in the reference LNG-fired power plant is designed to control emissions and ensure compliance with environmental standards. While LNG combustion is cleaner than coal or oil, it still produces nitrogen oxides (NO $_{\rm x}$), carbon monoxide (CO), and trace amounts of sulfur oxides (SO $_{\rm x}$) and particulates. To mitigate NO $_{\rm x}$ emissions, an ammonia-based flue gas cleaning system, such as Selective Catalytic Reduction (SCR), is employed. In the studied system, instead of using an adsorbent, ammonia (NH $_{\rm 3}$) is injected into the flue gas, reacting with NO $_{\rm x}$ to form harmless nitrogen (N $_{\rm 2}$) and water vapor.

Fig. 1 (b) shows the actual temperature-entropy (T-S) diagram of the Rankine cycle, which consists of the following processes;

- **1–2 (HPT):** High-pressure steam enters the turbine, undergoing an isentropic expansion process with negligible change in entropy.
- **2–3 (Reheating):** The steam is reheated to increase its energy content before entering the next stage of expansion.
- **3–4 (IPT):** Reheated steam enters the intermediate pressure turbine, where it again undergoes isentropic expansion with minimal entropy change.
 - **4–6 (Reheating):** Reheating at low pressure.
- **6–7 (LPT):** The steam enters the low-pressure turbine for isentropic expansion, with negligible entropy change.
- **7–8 (Condenser):** Ideally, heat is rejected at constant pressure in the condenser; however, in practice, there is a slight pressure drop due to piping resistance.
- **8–9 (CEP):** Isentropic compression process, a negligible entropy change occurs.
- **13–14 (BFWP):** The compression takes place under isentropic conditions, resulting in an insignificant entropy change.
 - 14-1 (Water Tube Boiler): Constant pressure process.

2.2. Analysis approach

The Balloki power plant operates under four different loading conditions depending on power demand. The operating conditions of power plants at 44.5 %, 78.75 %, 87.8 %, and 98.5 % load are shown in Tables 5 to 6, respectively. The temperature, pressure, and mass flow rate across each component are obtained from the power plant control room. This data is then input into the Engineering Equation Solver (EES) software to determine the enthalpy and entropy values for each component of the power plant. The calculated enthalpy and entropy values are utilized in equations to evaluate exergy efficiency, energy efficiency, exergy loss ratio, exergy destruction, and relative exergy destruction. Subsequently, algorithms are developed in Python using Google Colab to optimize energy and exergy efficiencies. Finally, a comparison is conducted between experimental and optimized values.

2.3. Analytical assumptions

Below are the assumptions for the energy-exergy analysis of the steam power plant:

1. The current study is conducted by maintaining steady-state conditions with the law of conservation of mass and energy

The power plant's steady-state operation, where the mass flow rate, energy input, and energy output stay constant across time, is assumed in the analysis. This assumption streamlines the computations and is valid for large-scale power plants operating under stable conditions. Start-up and shutdown phases are examples of transient impacts that are not considered since they bring dynamic fluctuations that require a different

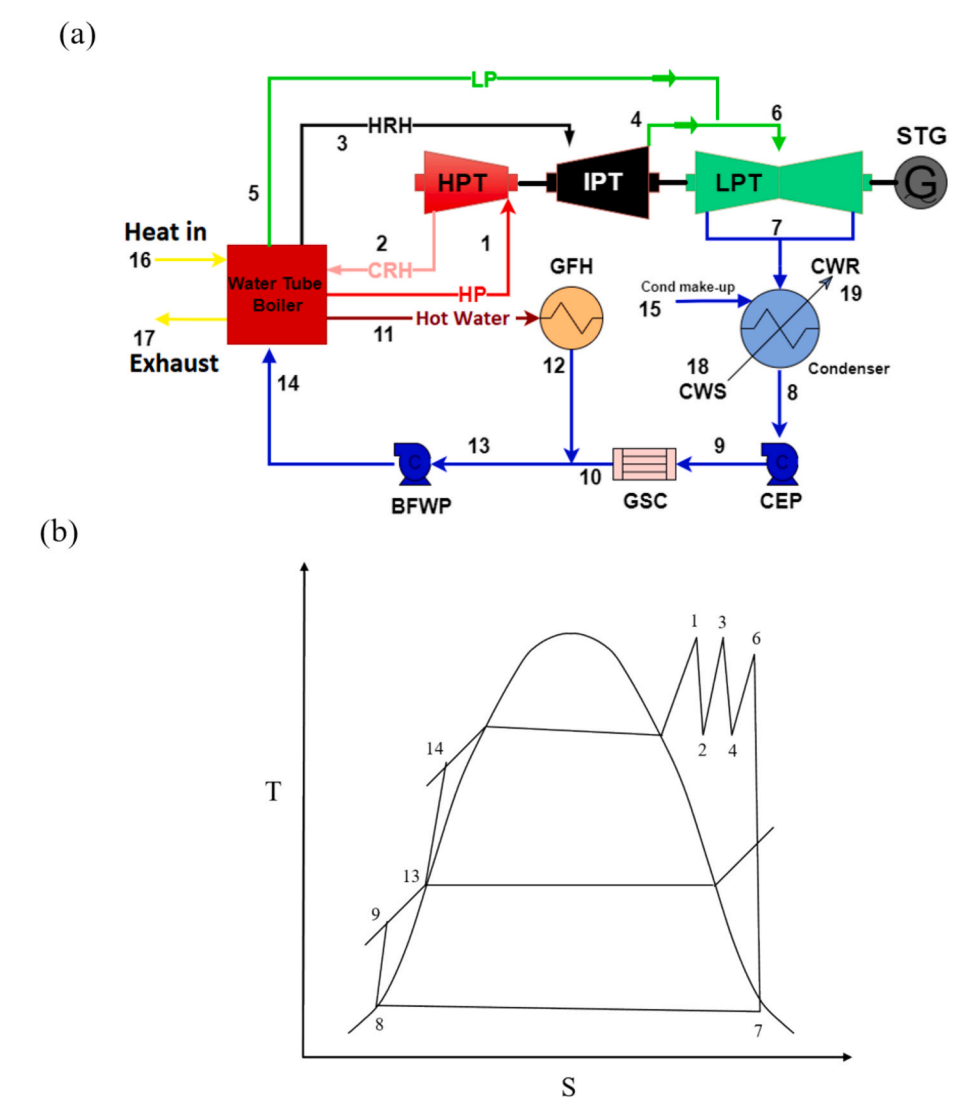


Fig. 1. (a) Schematic diagram of a power plant (b) Actual T-S diagram of the Rankine cycle.

Table 4Technical specifications of steam power plant.

Operating Conditions	Value/Specification	Unit
Type	Thermal Power Plant	_
Maximum Capacity	410.08 (NET)	MW
Rated Capacity	420.08 (Gross)	MW
Boiler Type	Fuel Gas Fired Boiler	_
Condenser Type	Two Pass Cross-Flow Heat Exchanger	_
Heater type	N/A	
Pump Type	Multistage High-Pressure Centrifugal	_
	Pump	
Rated heat rate	9607	kJ/
		kWh
Max mass flow rate at turbine	971	Tons/
inlet		hr
Rated mass flow rate at turbine	971	Tons/
inlet		hr
Turbine inlet pressure	164.8	Bar
Turbine inlet temperature	584.8	°C
Cooling Water Inlet	28.76	°C
Temperature		
Cooling Water Outlet	36.03	°C
Temperature		

modeling methodology.

2. Each component of the plant is deliberated as a control volume

Each constituent of the power plant (turbine, pump, boiler, and condenser) is regarded as a control volume, where energy and mass interactions take place across the boundaries. Such an approach is justified as it permits an accurate assessment of energy and exergy balances within each component without considering the interactions between components beyond the designated boundaries.

3. The change in potential and kinetic energies is neglected

The changes in kinetic energy due to velocity variations and potential energy due to altitude differences are assumed to be insignificant in comparison with the total energy in the steam cycle plant. Such an assumption is justified as the thermal energy and pressure variations dominate in Rankine cycle power plants, while height and velocity differences have a nominal influence on overall energy calculations.

4. The heat losses in pumps and turbines are neglected

Heat losses to the environment from the pump and turbine are assumed to be negligible. This presumption stems from the fact that

Table 5Operating conditions of power plant at 44.5 and 78.75% loading condition.

Point No.	44.50 % Lo	ad				78.75 % Load				
	Pressure	Temperature	Mass flow rate	Enthalpy	Entropy	Pressure	Temperature	Mass flow rate	Enthalpy	Entropy
	Bar	Kelvin	kg/s	kJ/kg	kJ/kg*K	Bar	Kelvin	kg/s	kJ/kg	kJ/kg*K
1	90	849	112.20	3574	6.89	140	850	181.40	3530	6.64
2	20	655	110	3207	7.06	31	648	180.70	3171	6.81
3	17.70	853	123.10	3647	7.70	29	843	200	3615	7.44
4	2.10	563	124.30	3051	7.83	3.40	553	200.70	3027	7.56
5	2.10	522	10.30	2968	7.68	3.10	535	18.30	2991	7.54
6	2.10	522	143.60	2968	7.68	3.20	548	218.30	3017	7.58
7	0.07	312.50	143.60	2572	8.26	0.09	317.30	218.30	2581	8.18
8	0.12	308.60	155.30	148.50	0.51	0.13	315.30	235	176.50	0.60
9	27	311.70	149.20	163.80	0.55	23	317.50	229	187.90	0.63
10	25	305.30	149.20	136.90	0.46	24.10	311.30	225	161.90	0.55
11	52.80	493	12.80	943.60	2.51	65	512	15.30	1032	2.68
12	52.80	397	12.80	523.70	1.56	65	412	15.30	588.3	1.72
13	27	311.20	161.90	161.70	0.54	24.30	324	243	215	0.71
14	180	324.20	161.90	229.10	0.71	194	336	241.90	279.20	0.85
15	0.50	302.80	5.60	124.20	0.43	0.50	303	8.30	125.10	0.43
16	1	943	833.30	1065	1.30	1	936	1325	1056	1.29
17	1	354.50	833.30	357.30	0.17	1	356	1305	358.9	0.18
18	3	306.20	20,833	138.70	0.48	3	307.90	20,833	145.80	0.50
19	2.30	309	20,733	150.30	0.52	2.30	312.60	20,833	165.40	0.56

Table 6Operating conditions of power plant at 87.80 and 98.80% loading condition.

Point No.	87.80 % Lo	oad				98.80 % Lo	ad			
	Pressure	Temperature	Mass flow rate	Enthalpy	Entropy	Pressure	Temperature	Mass flow rate	Enthalpy	Entropy
	Bar	Kelvin	kg/s	kJ/kg	kJ/kg*K	Bar	Kelvin	kg/s	kJ/kg	kJ/kg*K
1	150	857	202.40	3539	6.63	177	853	223	3503	6.52
2	34.50	653	201.20	3176	6.77	44	654.70	221.70	3161	6.65
3	28	885	223	3711	7.57	37.50	885	245.60	3703	7.43
4	4.80	578	229.40	3074	7.49	5.10	593	247.20	3105	7.52
5	4.50	560	20	3038	7.46	5.80	593	23.60	3103	7.46
6	3.30	553	243.90	3027	7.58	5.20	593	269.20	3104	7.51
7	0.09	319.90	243	2586	8.17	0.11	322	269.60	2589	8.11
8	0.12	317.60	253.90	186.10	0.63	0.12	319.50	278.60	194.10	0.66
9	23	319.70	245	196.90	0.66	23.80	321.60	270.60	204.90	0.68
10	22.80	313.70	250.60	171.80	0.57	22.80	316.50	270	183.50	0.62
11	64	528	16.70	1109	2.83	67	520	24.40	1070	2.76
12	64	428	16.70	656.80	1.88	67	449	24.40	748	2.09
13	31	322	271	207.20	0.68	33	323	303.10	211.50	0.70
14	207	332.40	255	265.40	0.81	203	333	300	267.50	0.82
15	0.50	302	6.70	120.90	0.42	0.50	301.20	69.40	117.60	0.41
16	1	913	1518	1026	1.25	1	910	1680	1022	1.25
17	1	358	1500	360.90	0.18	1	360	1680	363	0.19
18	3	307	20833.30	142.20	0.49	3	301.70	20833.30	120.10	0.42
19	2.30	314	20833.30	171.40	0.59	2.30	309.10	20833.30	150.90	0.52

contemporary power plants employ components that are well-insulated and have low external heat loss. Furthermore, this assumption is fair for real-world engineering calculations because most of the energy changes within these components take the form of work rather than heat dissipation.

5. The reference pressure is taken as 1.013 bar, and the reference temperature is taken as 25 $^{\circ}\text{C}$

Standard atmospheric conditions of 1.013 bar of pressure and 25 $^{\circ}\mathrm{C}$ of temperature are used as the reference state for exergy calculations. In thermodynamic analysis, this choice is frequently used to maintain uniformity and make comparisons with other studies more convenient. The ambient environment is represented by the reference state, which is used to assess the system's usable work potential.

2.4. Mathematical modeling

Each parameter of the plant is coded through EES software and validated through comparison with 'Real output data from the reference power plant' at different loading conditions. The mathematical models for all key components of the studied steam power plant cycle are briefly reported as:

2.4.1. Boiler

In the boiler, the fuel combustion provides heat energy to the fluid working in the boiler, which increases the pressure and temperature of the working fluid. The enthalpy & entropy of the fuel were calculated with equations (1) and (2), respectively. The mass flow rates at the inlet and exit of the boiler are given in Equation (3).

$$h = C_P \Delta T \tag{1}$$

$$s = C_p ln \frac{T}{T_o} \tag{2}$$

$$\dot{m}_{16}h_{16} + \dot{m}_{2}h_{2} + \dot{m}_{14}h_{14} = \dot{m}_{17}h_{17} + \dot{m}_{1}h_{1} + \dot{m}_{3}h_{3} + \dot{m}_{5}h_{5} + \dot{m}_{11}h_{11}$$
 (3)

The 1st Law efficiency was calculated as an output-input ratio. The output in the boiler is the working fluid flowing energy while the input is the fuel's energy. Ahmadi and Toghraie [94] explained the relation for ascertaining energy efficiency. Hence, the energy efficiency of the system is simply defined as the ratio of energy outputs and inputs. The expression for energy efficiency can be seen from equation (4):

$$\eta_1 = \frac{\dot{m}_1 h_1 + \dot{m}_3 h_3 + \dot{m}_5 h_5 + \dot{m}_{11} h_{11} - \dot{m}_2 h_2 - \dot{m}_{14} h_{14}}{\dot{m}_{16}(h_{16})} \tag{4}$$

The exergy destruction is the difference between the exergy of the fluid at the input and output points and is expressed as equation (5).

$$I_{Boiler} = X_1 + X_3 + X_5 + X_{11} + X_{16} - X_2 - X_{14} - X_{16}$$
(5)

2nd law efficiency is a ratio of the working fluid exergy difference to the exergy of the fuel and is expressed as equation (6).

$$\eta_2 = \frac{X_1 + X_3 + X_5 + X_{11} - X_2 - X_{14}}{X_{16} - X_{17}} \tag{6}$$

2.4.2. High pressure turbine

The heat losses in turbines are neglected as mentioned before so the turbine performance is calculated with its isentropic expansion work expressed as equations (7) and (8). Equation (8) is referred to in [95], including steam enthalpy at the turbine inlet and isentropic steam enthalpy at the turbine outlet as shown below:

$$W_{HPT} = \dot{m}_1(h_1 - h_2) \tag{7}$$

$$\eta_1 = \frac{\dot{m}_1(h_1 - h_2)}{\dot{m}_1(h_1 - h_{2s})} \tag{8}$$

Exergy destruction would be the difference between exergy entering and exergy leaving, along with the work done by the turbine. The performance in terms of exergy efficiency is calculated as the output-input ratio. The output is work that is achieved by the turbine, and the input is the exergy that is provided to the turbine, as in Equation (9). The exergy efficiency is expressed as Equation (10).

$$I_{HPT} = X_1 - X_2 - W_{HPT} (9)$$

$$\eta_2 = \frac{W_{HPT}}{X_1 - X_2} \tag{10}$$

2.4.3. Intermediate pressure turbine

The performance of the turbines is calculated based on their isentropic work, as the heat losses in the turbines are neglected. The work done by IPT is shown in Equation (11). The energy efficiency is expressed in terms of equation (12).

$$W_{IPT} = \dot{m}_3(h_3 - h_4) \tag{11}$$

$$\eta_1 = \frac{\dot{m}_3(h_3 - h_4)}{\dot{m}_3(h_3 - h_{4c})} \tag{12}$$

The exergy destruction is calculated as the difference between the turbine's entering exergy and leaving exergy, with the work output as expressed through Equation (13).

$$I_{IPT} = X_3 - X_4 - W_{IPT} (13)$$

The ratio of work with the exergy difference of the working fluid gives us the 2nd law efficiency as expressed by equation (14)

$$\eta_2 = \frac{W_{IPT}}{X_3 - X_4} \tag{14}$$

2.4.4. Low pressure turbine

Likewise, the performance of a low-pressure turbine is also evaluated with its isentropic work, as equations (15) and (16).

$$W_{LPT} = \dot{m}_6(h_6 - h_7) \tag{15}$$

$$\eta_1 = \frac{\dot{m}_6(h_6 - h_7)}{\dot{m}_6(h_6 - h_{7s})} \tag{16}$$

The difference between exergy entering the turbine and exergy leaving with work done gives us the exergy destruction value (equation (17). The ratio of work done by the turbine to the exergy difference of the working fluid gives us 2nd law efficiency, as in equation (18).

$$I_{LPT} = X_6 - X_7 - W_{LPT} (17)$$

$$\eta_2 = \frac{W_{LPT}}{X_6 - X_7} \tag{18}$$

2.4.5. Condensate extraction pump

A condensate extraction pump (CEP) extracts the condensed fluid from the condenser. The heat losses in pumps are neglected, so their performance is also evaluated with their isentropic work as expressed in equation (19).

$$W_{CEP} = \dot{m}_8(h_9 - h_8) \tag{19}$$

In the case of pumps, the input is the flow rate of working fluid, while the output is the power that is transmitted to the fluid. The energy efficiency in the case of CEP is expressed by equation (20).

$$\eta_1 = \frac{\dot{m}_8 (h_{9s} - h_8)}{W_{CEP}} \tag{20}$$

In pumps, input is the exergy at node 8 and the energy it uses to work. While the output pump is the exergy of the working fluid at node 9. The irreversibility in CEP is expressed by equation (21). The ratio of the exergy difference of the working fluid to work done by the pump gives us 2nd law efficiency, as in equation (22).

$$I_{CEP} = X_8 - X_9 + W_{CEP} (21)$$

$$\eta_2 = \frac{X_9 - X_8}{W_{CFP}} \tag{22}$$

2.4.6. Boiler feed water pump

A boiler feed water pump (BFWP) transfers working fluid toward the boiler. The heat losses in pumps are neglected so its performance is also evaluated with its isentropic work, as in equation (23). The energy efficiency is given by equation (24).

$$W_{BFWP} = \dot{m}_{13}(h_{14} - h_{13}) \tag{23}$$

$$\eta_1 = \frac{\dot{m}_{13}(h_{14s} - h_{13})}{W_{RFWD}} \tag{24}$$

In pumps, input is the exergy at the pump inlet, and the pump utilizes energy. While the output pump is the exergy of the working fluid at node 14. The irreversibility of BFWP can be calculated through equation (25). The ratio of the exergy difference of the working fluid to work done by the pump gives us 2nd law efficiency, as in equation (26).

$$I_{BFWP} = X_{13} - X_{14} + W_{BFWP} (25)$$

$$\eta_2 = \frac{X_{14} - X_{13}}{W_{BFWP}} \tag{26}$$

2.4.7. Gland steam condenser

A gland steam condenser (GSC) is the component of the power plant that captures and reuses the bleeding steam from the turbines and other components. The energy balance equation is given as equation (27). The energy efficiency is given as the ratio between output and input, as expressed by equation (28).

$$\dot{m}_9 h_9 = \dot{m}_{10} h_{10} + H l_{GSC} \tag{27}$$

$$\eta_1 = \frac{\dot{m}_{10}h_{10}}{\dot{m}_0h_0} \tag{28}$$

The exergy destruction is the difference between exergies at the inlet and outlet, and the 2nd law efficiency is the ratio between outlet and inlet exergies, as shown in equation (29). The exergy efficiency in the case of the gland steam condenser is given in equation (30).

$$I_{GSC} = X_9 - X_{10} (29)$$

$$\eta_2 = \frac{X_{10}}{X_0} \tag{30}$$

2.4.8. Gas fuel heater

The hot working fluid from the boiler is passed through a gas fuel heater (GFH) that increases the temperature of the fuel used in the combustion chamber, which is then added to the cold working fluid line to increase its temperature. GFH is a heat exchanger manufactured by Dalian Energas Gas-system Co. It is a category IV, NEN-type exchanger with 45 Bar and 250 °C maximum allowable pressure and temperature, respectively. The maximum allowable tube pressure and temperature are 93.1 Bar and 306.5/2C°. The shell has a capacity of 2081.5 L while the tubes have 679.1 L. The mass flow rate through the gas fuel heater is expressed through equation (31). The energy efficiency is given as the ratio between the output and input of GFH and expressed through equation (32).

$$\dot{m}_{11}h_{11} = \dot{m}_{12}h_{12} \tag{31}$$

$$\eta_1 = \frac{\dot{m}_{12}h_{12}}{\dot{m}_{11}h_{11}} \tag{32}$$

The exergy destruction is the difference between exergies at the inlet and outlet, and the 2nd law efficiency is the ratio between outlet and inlet exergies as expressed through equation (33). The exergy efficiency through GFH is expressed as equation (34).

$$I_{GFH} = X_{11} - X_{12} (33)$$

$$\eta_2 = \frac{X_{12}}{X_{11}} \tag{34}$$

2.4.9. Condenser

Cooling water is passed continuously through the condenser tubes that extract the energy of the working fluid. The energy balance and energy efficiency are given in equations (35) and (36), respectively:

$$\dot{m}_8 h_8 + \dot{m}_{19} h_{19} = \dot{m}_7 h_7 + \dot{m}_{15} h_{15} + \dot{m}_{18} h_{18} \tag{35}$$

The energy efficiency is given as the ratio of output and input. The condenser fluid extracts the heat as an output while the working fluid energy acts as an input.

$$\eta_1 = \frac{\dot{m}_{18}(h_{19} - h_{18}) - \dot{m}_{15}h_{15}}{\dot{m}_7(h_7 - h_8)}$$
(36)

The exergy destruction is the difference between exergies at the inlet and outlet, and the 2nd law efficiency is a ratio of the difference of condenser fluid exergies to the difference of working fluid (equation (37), and equation (8) shows the exergy efficiency of the condenser.

$$I_{GFH} = X_7 + X_{15} + X_{18} - X_8 - X_{19} (37)$$

$$\eta_2 = \frac{X_{19} - X_{18} - X_{15}}{X_7 - X_9} \tag{38}$$

2.5. Real plant's operational parameters

Balloki power plant is operated at four different loading conditions. Each component of the power plant possesses different pressure, temperature, mass flow rate, enthalpy, and entropy as detailed in Tables 5 and 6.

2.6. AI based approach using a random forest regression model

Random tree regression, a form of supervised learning, leverages multiple decision trees with random feature selection and bootstrap sampling to enhance predictive accuracy and prevent overfitting. The model demonstrates robustness, low sensitivity to outliers, and the capacity to make precise predictions for datasets. The random forest regression model operates by creating multiple decision trees from subsets of the training dataset, combining their predictions to form a robust and accurate model. Each decision tree is trained on a bootstrap sample with random feature subsets, and the overall model employs stopping criteria such as maximum depth, as illustrated in the architectural diagram in Fig. 2. The random forest regression model is employed for prediction, mitigating overfitting, and handling complex data by utilizing a 70:30 split between training and validation datasets. The model is built on bootstrap samples and incorporates input variables like enthalpy and temperature to predict energy and exergy efficiencies in a power plant. The model is developed in Python and executed on Google Colab. Hyper parameters, including 100 trees, maximum depth of 10, and specific split and feature criteria, are set, and the model's predictions for energy and exergy percentages are compared to experimental data, with average root mean square error (RMSE) and coefficient of determination (R2) computed for evaluation. The Random Forest model is trained on a Dell i7 laptop equipped with 8 GB of RAM, requiring approximately 2 h for completion. The model is configured with 100 trees, each constrained to a maximum depth of 10. Peak memory usage is observed at approximately 3 GB, which is well within the system's 8 GB RAM capacity. The computational cost is predominantly influenced by the complex decision-making processes inherent to each node within the ensemble of trees, despite the moderate size of the dataset.

RMSE (Root Mean Square Error) is the selected metric for evaluating the predictive performance of a Random Forest Regression (RFR) model in estimating the energy efficiency and exergy efficiency of a power plant for several reasons. The foremost reason is that both energy efficiency and exergy efficiency are critical factors in assessing the overall performance of a power plant, and any inaccuracies in their prediction can have significant operational and economic implications. RMSE, by penalizing larger errors more heavily, ensures that the model is sensitive to deviations in efficiency values, which is essential for capturing the nuanced variations in power plant performance. Additionally, the

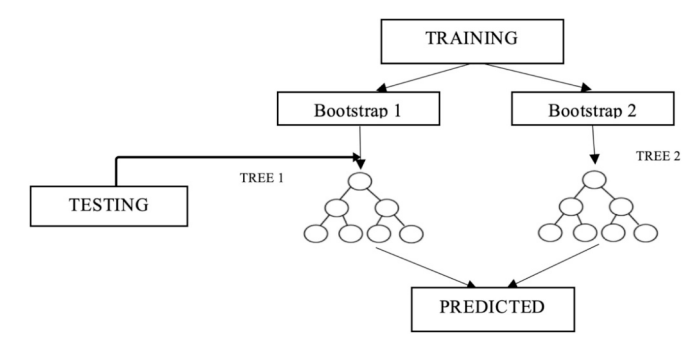


Fig. 2. Architecture diagram for the random forest regression model.

interpretability of RMSE, given that it is in the same units as the target variables (efficiency values), facilitates a clear understanding of how well the model aligns with the actual performance metrics relevant to energy and exergy efficiency. As Random Forests are often optimized based on minimizing squared errors, using RMSE and R² as the evaluation metric ensures consistency with the model's training objective. First, the model is trained for each combination of hyper parameters on the training dataset and evaluates its performance on a validation dataset using the evaluation metric, RMSE. The data set is split into a training set and a validation set by the ratio of 70:30. The model is trained by considering both input features and target features. After initial testing of the model, the importance of each feature is assessed. Features with higher importance contribute more to the model's predictions. The hyper parameters to develop the model are given in Table 7.

The model is then fine-tuned to optimize the parameters that result in the best performance on the validation set. This is based on minimizing RMSE values. Regression results are explained by RSME and R² values. RMSE is a measure of the average magnitude of errors between predicted and actual values. Specifically, RMSE calculates the square root of the average squared differences between predicted and actual values. The visualized diagram of actual versus predicted values highlights the performance of the model. High deviation can be an indication that the model needs to be improved further for better results. Hence, lower RSME indicated a better model. A benchmark can be established from the model results and can be used to optimize the performance of the power plant. The use of Random Forest Regression (RFR) for predicting energy efficiency and exergy efficiency in a power plant offers several advantages over alternative machine learning models. RFRM excels in capturing complex and nonlinear relationships between input features and efficiency metrics, making it well-suited for scenarios where traditional linear models may fall short. Its robustness to overfitting is particularly beneficial when dealing with noisy data or datasets with a large number of features, contributing to improved generalization on unseen data. Additionally, RFRM provides insights into feature importance, aiding in the interpretation of which factors significantly influence energy and exergy efficiency. The ensemble learning approach, combining multiple decision trees, enhances the model's overall robustness by mitigating individual tree biases and errors. The R2 value measures the proportion of variance in the actual data explained by the model.

3. Results and Discussions

The current study encompasses two main areas of investigation: experimental analysis and the enhancement of performance using artificial intelligence methods.

3.1. Experimental analysis

This section addresses key research questions, i.e., how mass flow rate, temperature, pressure, and loading conditions relate to metrics such as exergy loss ratio, exergy destruction, exergy efficiency, energy efficiency, and cycle efficiency.

Table 7Hyper parameters for RFR model.

Hyper parameters	Description
n estimator	100
max feature	sqrt
max depth	10
bootstrap	True
random state	42
min sample split	2
min sample leaf1	1

3.1.1. Energy efficiency

Energy efficiency in power plants is a critical factor in optimizing performance, reducing fuel consumption, and minimizing environmental impact. The current study evaluates energy efficiency by analyzing variations in power plant components under different loading conditions. Fig. 3(a) displays the variation in energy efficiency for different components of the power plant under distinct loading conditions. The results indicate that the energy efficiency slightly increases with the increase in load, a trend also observed in previous studies analyzing the energy systems. The energy balance analysis distinguishes energy inflow and outflow from the system, which is equal to the energy loss in the steam cycle. It is because of the lower isentropic efficiency or actual efficiency in comparison with the designated efficiency of a particular component. The lifespan of a component becomes short for continuous operations at lower efficiency. Recent studies have highlighted various strategies to enhance energy efficiency in thermal power plants. A 2022 study on hydroelectric plants in Brazil identified optimized equipment use and rationalized energy application as key strategies for achieving potential annual savings of 2,910 MWh [96]. Similarly, research on high-efficiency motors in thermal power stations emphasized their role in reducing electricity consumption and greenhouse gas emissions [97]. The energy analysis of Bokaro Thermal Power Station (210 MW capacity) [92] shows that the energy efficiency of the boiler, turbine, condenser, and pump is 88.92, 78.9, 44.3, and 72.9 %, respectively, along with 32.9 % overall energy efficiency. In another study on Jawa Power-YTL, Paiton, Indonesia [89], the energy efficiency of the boiler, turbine, condenser, and pump is 47.98, 54.66 to 84.53, 8.94, and 34.13 %, respectively. In the current study, the energy efficiency of the boiler, HPT, condenser, and BFWP was 85.26, 76.75, 69.52, and 22.76 %, respectively, along with 26.19 % of overall cycle efficiency at 44.5 % load. The energy efficiency of the boiler, HPT, condenser, and BFWP was 85.92, 77.23, 77.57, and 26.62 %, respectively, along with 27.90 % of overall cycle efficiency at 78.75 % load. The energy efficiency of the boiler, HPT, condenser, and BFWP was 90.82, 79.38, 80.33, and 30.44 %, respectively, along with 28.23 % of overall cycle efficiency at 87.80 % load. The energy efficiency of the boiler, HPT, condenser, and BFWP was 91.18, 79.99, 95.68, and 30.57 %, respectively, along with 30.45 % of overall cycle efficiency at 98.80 % load.

Moreover, energy leakage and isolated steam turbines cause energy losses. The steam enthalpy at the turbine exit possesses an inverse proportional relationship with turbine output, condenser pressure, steam quality, and moisture content. The moisture results in a drag force around the turbine, which decreases its output. The output of the turbine can be increased by decreasing the cooling water temperature in the condenser, which ultimately enhances the steam generation rate and energy efficiency. The condenser pressure directly impacts the steam temperature and the turbine output. However, it should be higher than the cooling medium temperature, as a lower steam temperature results in higher moisture content, leading to blade erosion and lower turbine efficiency. This issue can be addressed through steam reheating [98]. The condenser possesses maximum energy losses due to maximum energy input in the power cycle. Higher enthalpy drops around the turbine are mainly responsible for higher energy efficiency. As the pressure difference around the pump intake and outlet increases, the pump work also increases at the cost of lower power consumption, and ultimately turbine output starts increasing, which reflects on the higher thermal efficiency of the plant. The lower enthalpy drops around the turbine result in lower energy efficiency. By integrating AI-driven systems, energy losses can be minimized, and efficiency trends can be forecasted, allowing for proactive operational adjustments. Additionally, advanced heat recovery techniques, such as optimized HRSG systems, have been found to improve plant efficiency significantly. Furthermore, increasing reheat pressure and utilizing multiple reheating stages can mitigate moisture-related turbine losses, extending the lifespan of turbine blades. Improved insulation of boiler components, along with effective steam

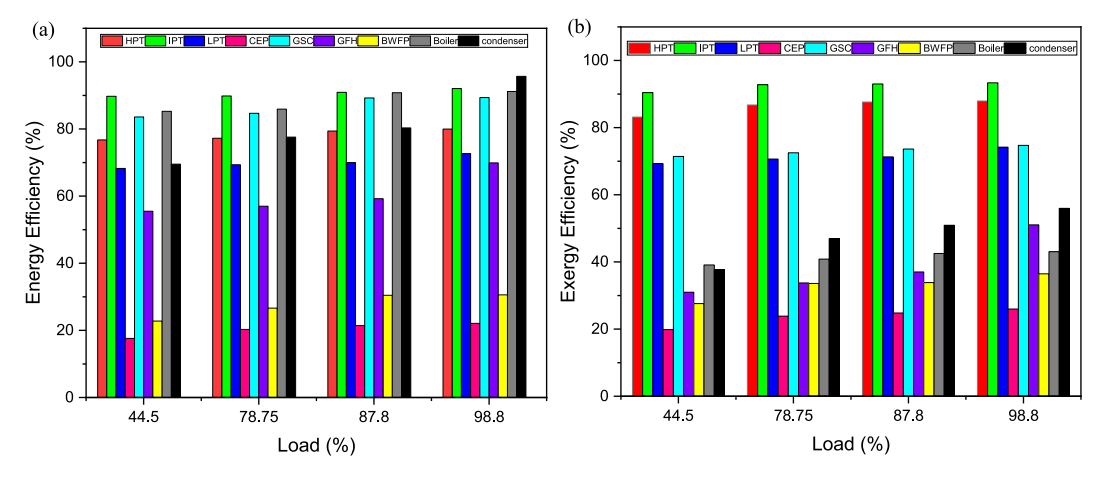


Fig. 3. Variation in (a) Energy efficiency, (b) Exergy efficiency for different components of the plant under distinct loading conditions.

leakage control measures, also contributes to minimizing energy dissipation. These enhancements collectively support higher overall plant efficiency, such as application of solar-assisted feedwater heaters [99], aligning with global trends in sustainable power generation.

3.1.2. Exergy efficiency

Fig. 3(b) displays the trend of exergy efficiency for multiple components of a steam powerplant concerning variation in loading conditions. It is observed that exergy efficiency is highest for the intermediate pressure turbine (IPT) and lowest for the condensate extraction pump (CEP). Moreover, exergy efficiency generally increases with increasing load, indicating a positive correlation between system performance and operational capacity. Exergy efficiency is a critical measure of a system's ability to convert available energy into useful work, considering both the quantity and quality of energy. Previous studies have emphasized that optimizing turbine operation parameters, such as steam pressure, temperature, and expansion ratios, significantly impacts exergy performance, e.g. Kaushik et al. [98] found that the highest exergy loss occurs in the boiler due to incomplete combustion, inadequate heat insulation, and entropy generation. Similarly, other studies found that combustion chambers, gas turbines, and heat recovery steam generators (HRSGs) contribute up to 83 % of total exergy destruction [22,23]. The intermediate pressure turbine is often designed for maximum exergy efficiency to ensure the effective conversion of thermal energy into mechanical work. This is achieved by optimizing the expansion process at intermediate pressure levels, reducing energy losses associated with excessive pressure differences and heat transfer inefficiencies. The IPTs can achieve exergy efficiencies as high as 97.34 %, demonstrating their role as a key component in improving overall plant efficiency [13]. Generally, the intermediate pressure turbine is designed for maximum exergy efficiency to ensure that the available thermal energy is effectively converted into useful mechanical work while considering various thermodynamic, operational, and engineering factors. IPT operates at an intermediate pressure level between the high-pressure (HP) and lowpressure (LP) turbines. This allows for a more controlled and efficient expansion of the steam. Operating at an intermediate pressure helps to minimize the energy losses associated with excessive pressure differences and excessive heat transfer. IPT discharges steam to the condenser where it is condensed back into liquid form. The pressure at which the steam is condensed affects the back pressure on the turbine. The lower condenser pressure can positively impact the turbine's performance. The increase in the turbine work output is because of rising steam temperature and pressure. Moreover, the impact of temperature on the cycle efficiency depends on pressure. Exergy efficiency in the boiler may decrease with increasing reference temperature [100]. Irreversibility is a consequence of friction between working fluid and hot combustible gases during their flow inside boiler pipes and ultimately results in lower

pressure. A slag in boiler pipes constrains heat transfer due to lower thermal conductivity.

3.1.3. Exergy loss ratio

The exergy loss ratio is a parameter that quantifies the proportion of available energy (exergy) lost due to irreversibilities in a system relative to the total exergy input. It helps identify inefficient components and optimize system performance. Mathematically, it is defined as the ratio of exergy destruction within a component to the total exergy input to the system. In a power plant, component efficiency is influenced by the operating load. At lower loads, efficiency decreases due to higher relative heat losses and the off-design performance of turbines, boilers, and heat exchangers. Conversely, at higher loads, efficiency improves as components function closer to their design conditions, leading to lower specific fuel consumption and reduced exergy destruction. For instance, turbines achieve peak efficiency at full load by operating near their design parameters. However, at partial loads, efficiency declines due to increased steam leakage, lower steam flow rates, and higher mechanical losses relative to power output. To enhance overall plant efficiency and minimize exergy losses, it is important to optimize load distribution and ensure components operate within their ideal range.

Fig. 4(a) represents the variation in the exergy loss ratio for different components of the plant under varying loading conditions. It is observed that the exergy loss ratio decreases for the plant's components with increasing percentage load. As the load increases, the components become more efficient as they perform at rated capacity [101]. Specifically, as the load increases, the components are subject to conditions closer to their design specifications, optimizing their performance. This efficiency improvement is a result of both higher load and mass flow rates, which are tightly interlinked. Fig. 4(a) shows that a higher mass flow rate of steam causes a reduction in the exergy loss ratio. At lower load levels, where components operate below their rated capacity, efficiency suffers, and any deviation from the design point (either below or above rated conditions) results in less efficient performance. When the load increases, the mass flow rate rises, improving the overall performance of the system. Higher mass flow rates, particularly of steam, enhance the system's thermodynamic efficiency by improving heat exchange processes and reducing losses. This led to a lower exergy loss ratio, reflecting a better conversion of available energy into useful work. The exergy loss ratio is the ratio of losses in useful energy to the available useful energy, i.e., exergy. The total exergy loss in the turbine is lower than the condenser because of the exergy transfer into the cooling water. This indicates that, despite energy being lost in both the turbine and the condenser, the cooling process in the condenser results in more effective energy dissipation, thus lowering the exergy loss relative to the available exergy. At higher evaporation pressures, the irreversibility of the pump, condenser, and turbine is generally higher, but the evaporator

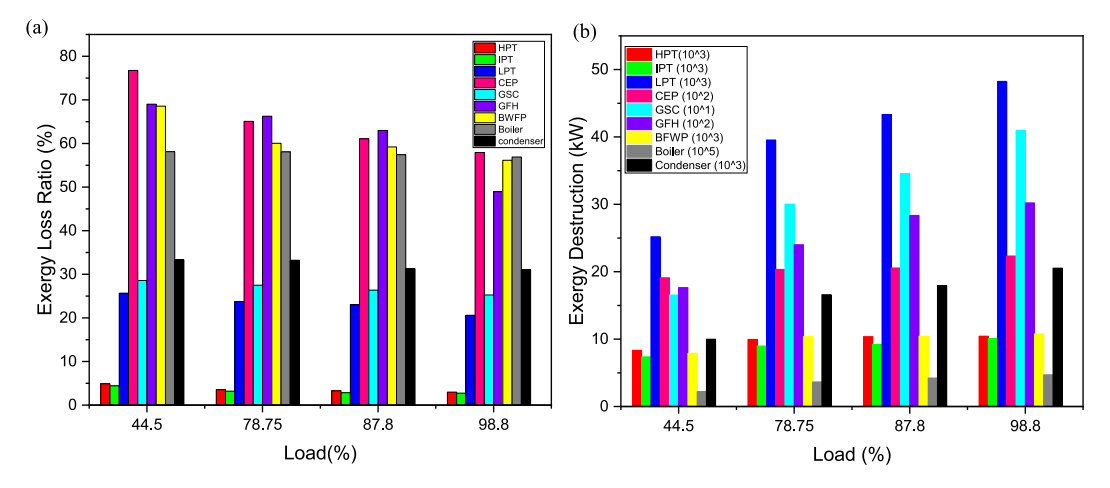


Fig. 4. Variation in (a) Exergy Loss Ratio, (b) Exergy destruction for different components of the plant under distinct loading conditions.

shows the opposite trend. The increment in evaporator pressure improves overall exergy efficiency as the reduction in the irreversibility of the evaporator is higher than that of the pump, turbine, and condenser.

The exergy destruction in the condenser is inversely proportional to exergy efficiency. As inlet air pressure decreases, the exergy efficiency increases, and the combustion efficiency decreases. This dynamic is critical in understanding the underlying thermodynamic behavior of the plant, as exergy analysis reveals trends and insights that traditional energy analysis may not highlight. The analysis of results shows that the condenser, despite its apparent higher energy losses, experiences greater exergy losses in the boiler. This disparity emphasizes the importance of exergy analysis in highlighting irreversibilities in the system that might not be as apparent through conventional energy-based evaluations. By identifying where exergy destruction occurs most significantly, the areas for improvement can be prioritized to enhance the overall efficiency of the thermodynamic system. Energy analysis depicts maximum energy losses in the condenser, but exergy analysis represents maximum losses in the boiler. The energy efficiency of an adiabatic turbine decreases with a decrease in pressure ratio, but exergy efficiency increases with a decrease in pressure ratio and an increase in cycle temperature. Except condenser, all other components of the steam power plant experience higher exergy loss due to the increase in atmospheric temperature. The higher difference between the system and environmental temperature creates an adverse impact on system performance. Factors like energy loss from flue gases, heat dissipation, and incomplete combustion significantly contribute to higher energy loss from the boiler. However, factors like flue gas leakage contribute towards maximum energy loss due to an increase in temperature difference between the atmosphere and the system. The huge amount of energy loss in the boiler is mainly because of flue gas leakage, incomplete combustion, and heat dissipation from the boiler surface. The energy losses from turbines and pumps are primarily caused by mechanical friction. Therefore, improvements should be made in reducing exergy losses for the optimized performance, such as air preheating, higher fuel-to-air ratio, and oxygen enrichment [102].

3.1.4. Exergy destruction

Fig. 4(b) highlights that the boiler is responsible for the highest exergy destruction in the plant, primarily due to the chemical reactions within the combustion chamber and the large temperature difference between the combustion gases and the working fluid. This temperature gradient leads to significant entropy generation, increasing exergy losses. Exergy destruction in the boiler is directly proportional to the combustion rate, as higher combustion rates exacerbate temperature differences, leading to greater inefficiencies. The inefficient combustion, heat transfer losses, and entropy generation are the primary factors that

contribute to boiler exergy destruction. Regular combustion optimization, including proper air-fuel ratio tuning and adjustment in the burner, is indispensable to reduce boiler exergy destruction. The periodic cleaning of the surface of heat exchangers and the application of advanced boiler tube coatings prevent scaling and fouling. Moreover, the appropriate insulation and sealing leaks significantly reduce heat dissipation, while real-time steam quality monitoring certifies optimal temperature and pressure. A proper boiler maintenance schedule, including water treatment and blowdown, prevents corrosion and scaling, which ultimately extends the lifespan of the boiler. The automatic feedwater control and AI-based predictive maintenance can also optimize boiler performance. Although the feed water heater can reduce exergy destruction by preheating the feedwater, its effect is limited due to the fundamental inefficiencies in the boiler's combustion process. Higher flue gas flow rates at the boiler exit result in increased exergy destruction, driven by greater entropy generation. In the turbine, key factors such as the pressure ratio, total reheat stages, and pressure drop significantly impact exergy losses. A lower pressure ratio reduces work output, leading to higher exergy destruction [21]. However, increasing the number of reheating stages helps to mitigate exergy destruction by optimizing energy conversion. Meanwhile, pressure drops increase entropy generation, exacerbating exergy losses and reducing overall system efficiency. The exergy destruction rate in the boiler decreases as the gas turbine inlet temperature increases. This is because higher inlet temperatures allow for more efficient combustion and energy conversion, reducing thermal irreversibilities and, consequently, exergy losses. At half load, increasing the condenser vacuum pressure reduces the relative exergy destruction in both the turbines and condensers. This improvement is due to the enhanced thermodynamic conditions, which lead to more efficient expansion in the turbine and reduced irreversibilities in the condenser. While exergy destruction in the condenser decreases, the turbine experiences an increase in exergy destruction as the condenser pressure drops.

The overall effect of reduced exergy destruction in the condenser outweighs the increase in the turbine, leading to an overall improvement in both energy and exergy efficiencies. At full and half loads, the increase in steam temperature contributes to a reduction in exergy destruction in both the boiler and turbine. This is because higher steam temperatures improve the heat transfer efficiency, reducing irreversibilities during energy conversion. The combined effects of higher steam temperature and optimized pressure conditions ultimately result in improved plant efficiency, both in terms of energy and exergy. This highlights the crucial role of thermodynamic optimization in enhancing the performance of power plant systems. Exergy destruction is a result of entropy generation due to sharper temperature differences, chemical reactions, higher temperature differences, and heat loss to the

environment [103]. The higher isentropic efficiency in the case of IPT results in lower exergy destruction. A higher isentropic efficiency is due to lower temperature and pressure steam with a lower mass flow rate. The degree to which an actual turbine resembles ideal (isentropic) expansion is measured by its isentropic efficiency. Higher isentropic efficiency implies less irreversibility and less energy destruction because it results in less deviation from the ideal process. Isentropic efficiency improves when irreversibility like friction, turbulence, and heat loss decrease. In intermediate-pressure turbine (IPT), steam expansion takes place at lower pressures and temperatures than in high-pressure stages. The lower mass flow rates and lower steam density result in lower frictional losses and heat transfer irreversibilities, which contribute towards higher efficiency. The isentropic efficiency depends on multiple factors like operating conditions, blade design of the turbine, and flow path optimization rather than sole mass flow rates.

3.1.5. Relative exergy destruction

Fig. 5 shows relative exergy destruction across power plant components under varying load conditions. The boiler experiences the highest exergy destruction due to the significant irreversibilities inherent in the combustion process and the large temperature difference between the combustion gases and the working fluid. This temperature gradient increases entropy generation, resulting in higher exergy losses. On the other hand, the gas-steam condenser (GSC) exhibits the lowest exergy destruction, primarily because of the minimal temperature change between its inlet and outlet, reducing irreversibility and entropy generation. This highlights the importance of temperature gradients in determining exergy losses in power plant systems. Fig. 5 (a) shows the relative exergy destruction ratio for inspected components at a 44.50 % loading condition. The boiler has a maximum relative exergy destruction of 78.1 %, and GSC possesses the least relative exergy destruction of 0.1 % at a 44.50 % loading condition. Fig. 5 (b) shows the relative exergy destruction ratio for inspected components at 78.75 % loading condition. The boiler has a maximum relative exergy destruction of 80.4

%, and GSC possesses the least relative exergy destruction of 0.1 % at 78.75 % loading condition. Fig. 5 (c) shows the relative exergy destruction ratio for inspected components at 87.80 % loading condition. The boiler has a maximum relative exergy destruction of 81.5 %, and GSC possesses the least relative exergy destruction of 0.1 % at 87.80 % loading condition. Fig. 5 (d) shows the relative exergy destruction ratio for inspected components at 98.80 % loading condition. The boiler has a maximum relative exergy destruction of 81.9 %, and GSC possesses the least relative exergy destruction of 0.1 % at 98.80 % loading condition. The boiler has the highest exergy destruction ratio, ranging from 78.1 to 81.9 %, due to chemical reactions under four different loading conditions. The second-highest exergy destruction ratio ranges from 8.3 to 8.9 % in LPT due to exergy loss to surroundings, lower quality steam, and lower isentropic efficiency. The rest of the exergy destruction ratios include 3.4 to 4.5 % in the condenser, 1.8 to 2.9 % in the HPT, 1.8 to 2.6 % in IPT, 0.4 to 0.7 % in CEP, 0.1 % in GSC, 0.5 to 0.6 % in GFH, and 1.8 to 2.7 % in BFWP. The lower exergy destruction for pumps and turbines is fundamental because of isentropic efficiencies, which involve design considerations and tribological aspects. The design considerations have the highest influence on energy efficiency. However, the economic aspects and spatial constraints should be taken care of during the design of efficient heat exchangers with higher surface area. The irreversibility rate of the condenser is decreased when the ambient temperature increases, as the temperature difference between the steam and cooling air temperature increases. It ultimately results in higher exergy efficiency and lower exergy destruction. The exergy efficiency increases with the increase in load. Therefore, it is suggested to run the powerplant at full loading conditions. The boiler is the source of maximum exergy destruction, so there is a lot of potential for improvement in the effective performance of the boiler. LPT is the second-largest source of exergy destruction. The work potential of the turbine can be improved. The temperature difference between steam and flue gases reduces significantly through increasing reheat pressure and the number of heaters, which ultimately improves turbine work potential. The optimum mass

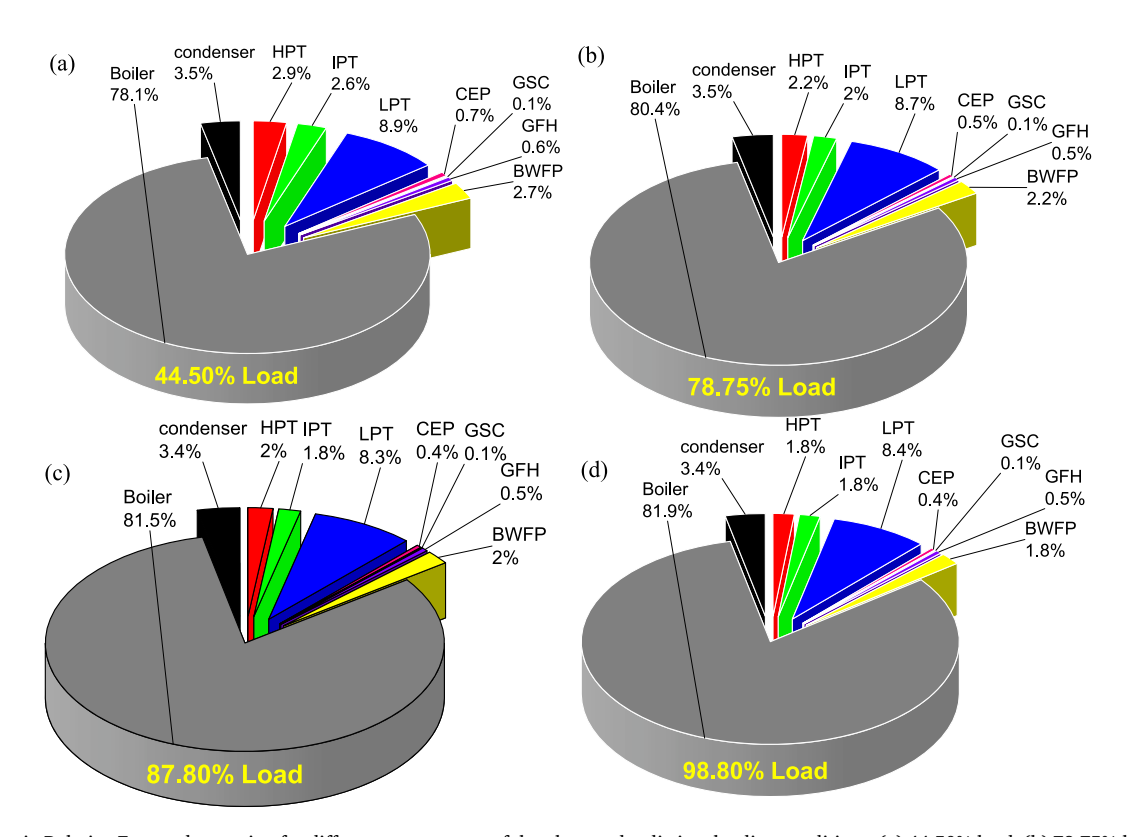


Fig. 5. Variation in Relative Exergy destruction for different components of the plant under distinct loading conditions: (a) 44.50% load, (b) 78.75% load, (c) 87.80% load, (d) 98.80% load.

fraction during reheating needs to be selected, as energy/exergy efficiency decreases for a higher mass fraction [104].

3.1.6. Plant's efficiency

Fig. 6 shows the plant cycle's efficiency, including both energy and exergy, under different loading conditions. Exergy efficiency is based on the quality of heat energy input. It is given based on the 2nd law of thermodynamics. Some of the heat must be rejected by the environment or sink. So, efficiency calculation considers the maximum potential of heat energy input by multiplying Q_{in} by $\left(1 - \frac{T_L}{T_H}\right)$. This will result in a

lower available heat input compared to that calculated using the First Law of Thermodynamics efficiency formula. This explains why exergy efficiency remains higher than energy efficiency across all load conditions [24]. The trends for exergy efficiency are higher than those of energy efficiency, mainly because exergy efficiency accounts for system irreversibilities and energy quality. The higher in-cylinder pressure and temperature at higher loading conditions promote combustion efficiency. Enhanced combustion at higher loads reduces irreversibilities, leading to lower heat losses and improved exergy efficiency. Moreover, exergy efficiency is a measure of the useful work potential of fuel, whereas energy efficiency accounts for the ratio of output energy and input energy without accounting for energy quality. At higher loading conditions, the energy proportion converted to useful work increases, which boosts exergy efficiency more as compared to energy efficiency. At 44.5, 78.75, 87.8, and 98.8 % load, the energy efficiency is 26.19, 27.9, 28.23, and 30.45 %, respectively. The exergy efficiency at 44.5, 78.75, 87.8, and 98.8 % load is 31.33, 35.19, 35.3, and 36.04 %, respectively. Moreover, these values are very well supported in previous literature [105,106]. It is clear from the figures that cycle efficiencies, including both exergy and energy, usually increase with the increasing value of load. The reheat pressure ratio is directly proportional to the plant's efficiency. By incrementing the reheat pressure ratio for turbines, fuel consumption also increases in the reheater, and the expansion ratio in LPT gets reduced, consequently, EGT increases, and creates a positive impact on the plant's efficiency [107]. Energy efficiency deals with total energy balance only; however, exergy efficiency deals with both irreversibilities and energy quality relative to the dead state. Energy efficiency is a more competent parameter to evaluate the power plant's performance than energy efficiency. It is because it considers how much input energy is transformed into useful work, along with the losses identification in respective areas. The dead state is such a condition of

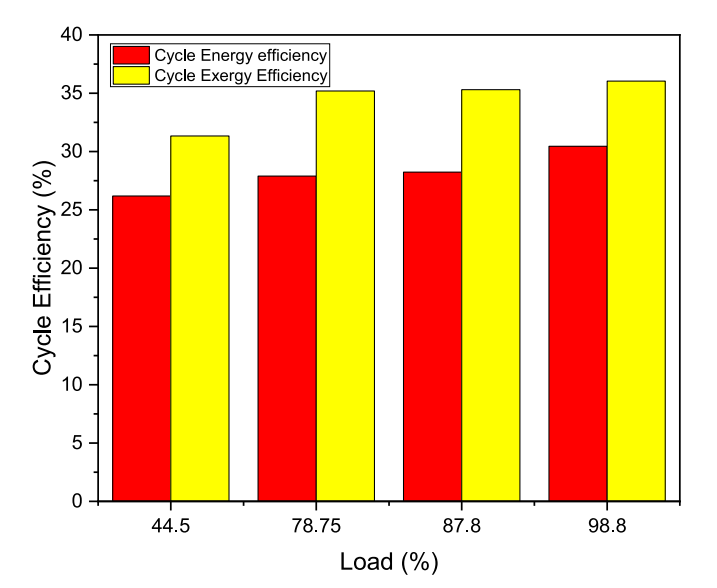


Fig. 6. Variation in Cycle efficiency (Energy and Exergy) for different components of the plant under distinct loading conditions.

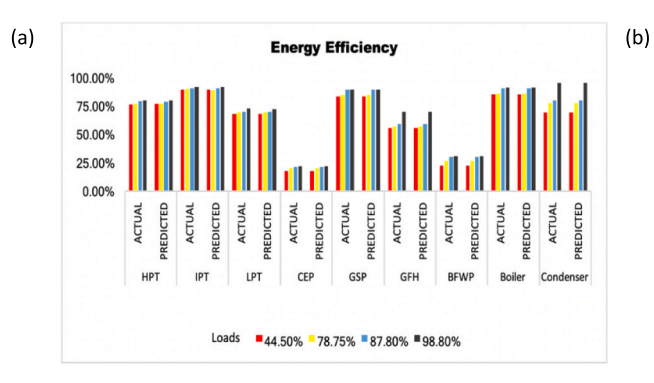
the power plant when the working fluid (steam) and all other system components are in general equilibrium with the environment. It can be inferred that the system does no useful work because of no pressure, temperature, or chemical potential difference between the system and the surroundings. For dead state characterization, the temperature (T_0) is 25 °C or 298 K, the pressure (T_0) is taken as 1 atm or 101.325 kPa, and the working fluid exists as saturated liquid at T_0 and T_0 . The dead state serves as a reference point to ascertain exergy efficiency, exergy loss ratio, and exergy destruction. The comparison between actual operating conditions and the dead state of the power plant highlights the areas where exergy losses are significant due to irreversibilities.

3.2. AI approach

A random tree regression model is developed to forecast energy efficiency and exergy efficiency by leveraging factors such as temperature, enthalpy, entropy, and mass flow rate. The model performance is assessed using the root mean square error (RMSE) metric. The dataset is split into training and testing sets in a 70:30 ratio. The training data is utilized for model construction and fine-tuning, while the test data is employed for making predictions. After the model is completed using the training data, it is evaluated using the test data to predict energy efficiency and exergy efficiency under various load conditions. The results indicate that the average RMSE for energy efficiency is 0.0852, while the average RMSE for exergy efficiency is 0.068. These RMSE values suggest that the model demonstrates reasonable accuracy in predicting both energy and exergy efficiency for the power plant. Fig. 7 (a) illustrates the comparison between the experimental and the predicted values of energy percentage at different stages of the plant i.e., at 45 %, 79 %, 88 %, and 99 % loads. The model efficiency closely matches the experimental values, with the least discrepancy observed at 99 % load, where the energy efficiency percentage is maximized. The overall average RMSE for energy efficiency percentage remains at 0.0852. In Fig. 7(b), a comparison between the experimental and the predicted values of percentage energy at various stages of the plant is reported. The comparison is also made for performance under 45 %, 79 %, 88 % load, and 99 % loads. The overall average RMSE for the energy efficiency percentage is 0.068. By analyzing the predicted results against experimental data, the coefficient of determination (R2) is computed for various stages of the power plant. Remarkably, the overall average R² value is 0.869 for energy analysis and 0.987 for exergy analysis.

Fig. 8 presents a comparison of experimental and predicted values for both energy efficiency and exergy efficiency at specified load levels of 44.5 %, 78.755 %, 87.8 %, and 98.8 %. The model's ability to yield low RMSE values underscores its effectiveness in accurately assessing and forecasting energy and exergy efficiency. Consequently, this model holds promise for precise predictions of the power plant efficiencies, enabling optimization of plant operations. Nonetheless, it is worth noting that further enhancements could be achieved by incorporating a more extensive dataset for future applications.

The performance of the predictive model, the Random Forest Regression (RFR) model, is evaluated using two key statistical metrics, mainly the coefficient of determination (R²) and the root mean square error (RMSE). The R² value quantifies the proportion of variance in the actual data that the model can explain, with values closer to 1 indicating a stronger correlation between predicted and actual values. A high R² suggests that the model can capture underlying patterns effectively, making it a reliable tool for prediction. Meanwhile, RMSE measures the average deviation of the predicted values from the actual values, with lower values indicating higher accuracy and precision. Fig. 9 compares the actual and predicted results for energy efficiency for different power plant stages through R² and RMSE. Fig. 9 (a) shows that the highpressure turbine (HPT) achieved an R2 of 0.9643 and an RMSE of 0.097, demonstrating strong predictive accuracy but slightly higher error compared to other stages. The intermediate-pressure turbine (IPT) exhibited an R² of 0.9587 and an RMSE of 0.092, indicating reliable



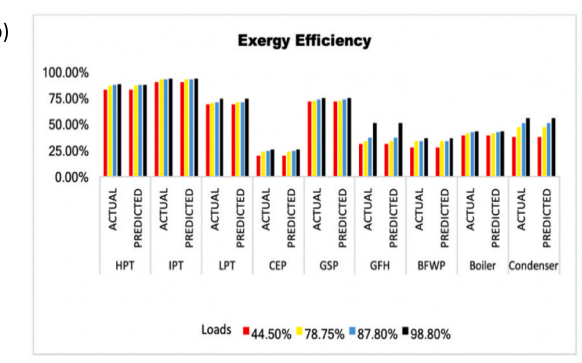


Fig. 7. Comparison of actual values with predicted values by the model for (a) energy efficiency and (b) exergy efficiency.

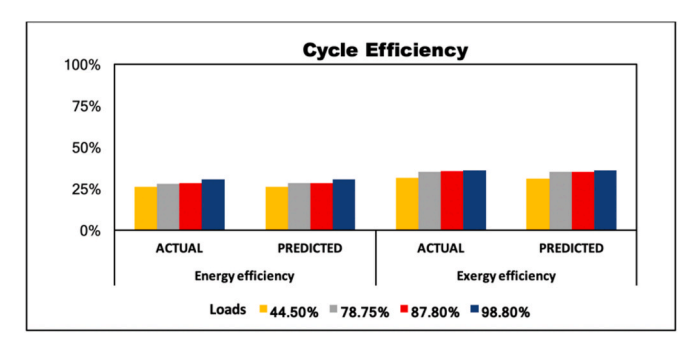


Fig. 8. Comparison of experimental values with predicted values of cycle efficiency of the plant.

performance with minimal deviation (see Fig. 9 (b). The low-pressure turbine (LPT) followed a similar trend, with an R2 of 0.9569 and an RMSE of 0.084, reinforcing the model's ability to predict efficiency with a small margin of error (see Fig. 9 (c)). Fig. 9 (d) shows that the condensate extraction pump (CEP) performed well, with an R² of 0.9599 and an RMSE of 0.091, reflecting a strong correlation between actual and predicted values. Fig. 9 (e) displays that the gland steam condenser (GSC) achieved one of the highest R² values at 0.9823 with an RMSE of 0.082, highlighting exceptional model accuracy. Fig. 9 (f) shows that the gas-fuel heater (GFH) also showed excellent predictive capability, with an R² of 0.9911 and an RMSE of 0.084. The boiler feed water pump (BFWP) (see Fig. 9(g)) and the boiler (see Fig. 9(h)) itself demonstrated high accuracy, with R² values of 0.9892 and 0.9882, respectively, and RMSE values of 0.076 and 0.079, ensuring reliable efficiency predictions. Fig. 9 (i) shows that the condenser exhibited the best performance, with the highest R² of 0.997 and the lowest RMSE of 0.062, confirming near-perfect predictive accuracy. Overall, the model demonstrated strong predictive capability across all stages, with consistent performance and minimal error in estimating energy

Fig. 10 evaluates the model results for exergy efficiency for different power plant stages. Fig. 10 (a) shows that the high-pressure turbine (HPT) achieved an R^2 of 0.9576 and an RMSE of 0.08, indicating strong predictive reliability with minor deviations. Fig. 10 (b) shows improved performance with an R^2 of 0.9794 and an RMSE of 0.081, reflecting a well-trained model with minimal error in the case of the intermediate-pressure turbine (IPT). Fig. 10 (c) shows that the low-pressure turbine (LPT) exhibited excellent predictive capability, with an R^2 of 0.9943 and an RMSE of 0.064, signifying high correlation and accuracy. Fig. 10 (d) shows that the condensate extraction pump (CEP) displayed exceptional results, with an R^2 of 0.9956 and an RMSE of 0.063, suggesting good alignment between actual and predicted values. Fig. 10 (e) shows that the gland steam condenser (GSC) attained an R^2 of 0.9784 and an RMSE of 0.078, highlighting robust model performance. The gas-fired heater

(GFH) demonstrated outstanding accuracy, with an R² of 0.9979 and an RMSE of 0.059, making it one of the best-performing stages (see Fig. 9 (f)). Similarly, the boiler feed water pump (BFWP) (see Fig. 10 (g)) and the boiler (see Fig. 10 (h)) itself showed high reliability, with R² values of 0.994 and 0.9916, respectively, and corresponding RMSE values of 0.062 and 0.064. Fig. 10 (i) shows that the condenser achieved the highest precision, with an R² of 0.996 and an RMSE of 0.061, confirming high model accuracy. Overall, the model demonstrated consistent and reliable predictive performance across all stages, ensuring accurate exergy efficiency estimations with minimal deviations.

4. Conclusions

The present study aims to investigate and predict the performance of a 400 MW steam power plant operating on the Rankine cycle through a combined exergy-energy analysis and an artificial intelligence-based random forest regression model.

The following conclusions can be drawn from the present study:

- The efficiency and performance of the turbine are significantly influenced by factors such as steam quality, superheat, and reheat pressure at the outlet of a low-pressure turbine. Additionally, there is an opportunity to explore the potential of utilizing waste flue gas from the power plant for practical purposes, which can contribute to sustainability. Furthermore, to reduce exergy losses originating from the boiler, minimizing the temperature difference between the system and the environment is essential while increasing the heat transfer area. This step can lead to improved overall system efficiency.
- The exergy efficiencies are calculated as 31 %, 35 %, 35 %, and 36 % at load conditions of 44.50 %, 78.75 %, 87.85 %, and 98.80 %, respectively. In contrast, the corresponding energy efficiencies were found to be 26 %, 28 %, 28 %, and 30 %. The studied results highlight significant room for enhancement, and it is noteworthy that the energy efficiencies are lower than the exergy efficiencies at various loading conditions, underscoring the importance of exergy efficiency, which considers the quality of energy and its efficient conversion into useful work. Even in cases where the overall energy input is substantial, a process that effectively harnesses high-quality energy can achieve high exergy efficiency. Furthermore, the boiler serves as a source of maximum exergy destruction due to irreversibility associated with the combustion process. The inlet air temperature and excess air fraction significantly affect exergy destruction in the combustion chamber. However, preheating air can reduce exergy destruction, increasing the fuel-to-air ratio and evaporator pressure. Although the superheating of steam increases the plant's efficiency, it also limits the safety limit of the plant due to metallurgical constraints. However, the boiler pressure increases thermal efficiency, but it also increases the moisture content in

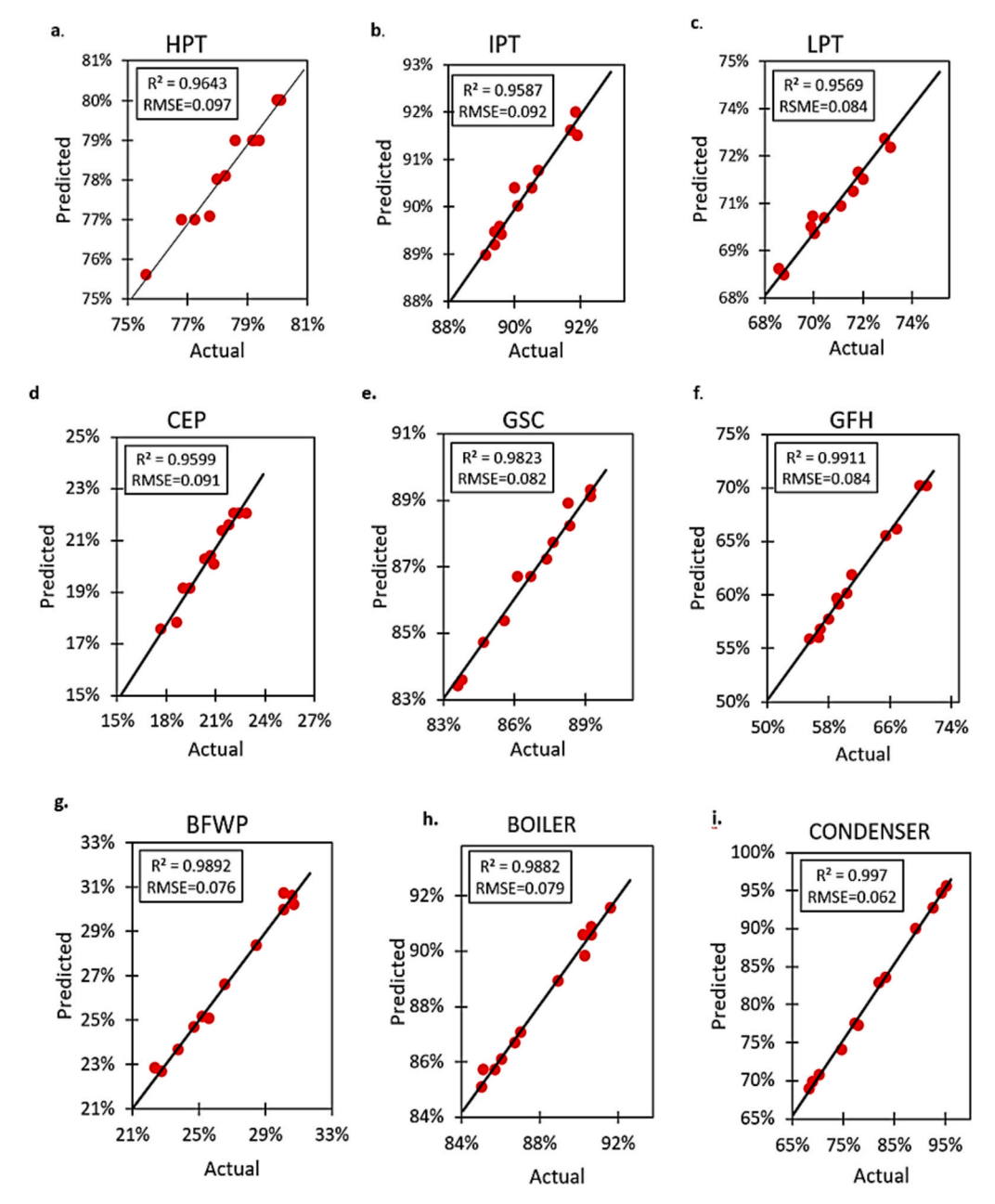


Fig. 9. Model performance for energy efficiency at different stages of the plant: (a) HPT, (b) IPT, (c) LPT, (d) CEP, (e) GSC, (f) GFH, (g) BFWP, (h) Boiler, (i) Condenser.

steam, which may erode turbine blades. Steam reheating can reduce moisture problems.

• IPT showed maximum energy efficiency, followed by GSP, Boiler, and condenser. However, the CEP showed the lowest energy efficiency, followed by BFWP. The energy efficiency for IPT is 89.75, 89.83, 90.94, and 92.05 % at 44.50, 78.75, 87.80, and 98.8 % loading conditions. The energy efficiency for CEP is 17.6, 20.29, 21.43, and 22.08 % at 44.50, 78.75, 87.80, and 98.8 % loading conditions. Similarly, the IPT showed maximum exergy efficiency, followed by GSP, and CEP showed the least exergy efficiency, followed by BFWP. The exergy efficiency for IPT is 90.44, 92.79, 93.0, and 93.37 % at 44.50, 78.75, 87.80, and 98.8 % loading conditions. The exergy efficiency for CEP is 19.84, 23.86, 24.79, and 25.98 % at 44.50, 78.75, 87.80, and 98.8 % loading conditions. Both energy and exergy analysis show that IPT is running at maximum potential, however, the CEP possesses energy losses. The frictional losses in

bearings and seals in CEP, and cavitation due to lower suction pressure, may result in pump impeller erosion, air ingress, and fouling in pipelines. Regular monitoring of CEP is required for the optimal performance of the plant, resulting in higher electrical production. Furthermore, the improvement in heat recovery systems and reduction in exergy destruction may also result in higher electrical production of plants.

• The optimum number of feed water heaters should be used in the power plant as more heaters will raise the boiler temperature and reduce fuel consumption in the boiler. The plant's efficiency decreases with the increase in atmospheric temperature. The heat losses are higher for the lower temperature difference between the system and the environment. The boilers can be improved through chemical loop combustion or effective utilization of insulated materials and piping. Inlet pressure, temperature, construction design, and materials can improve turbine performance. Condensers can be

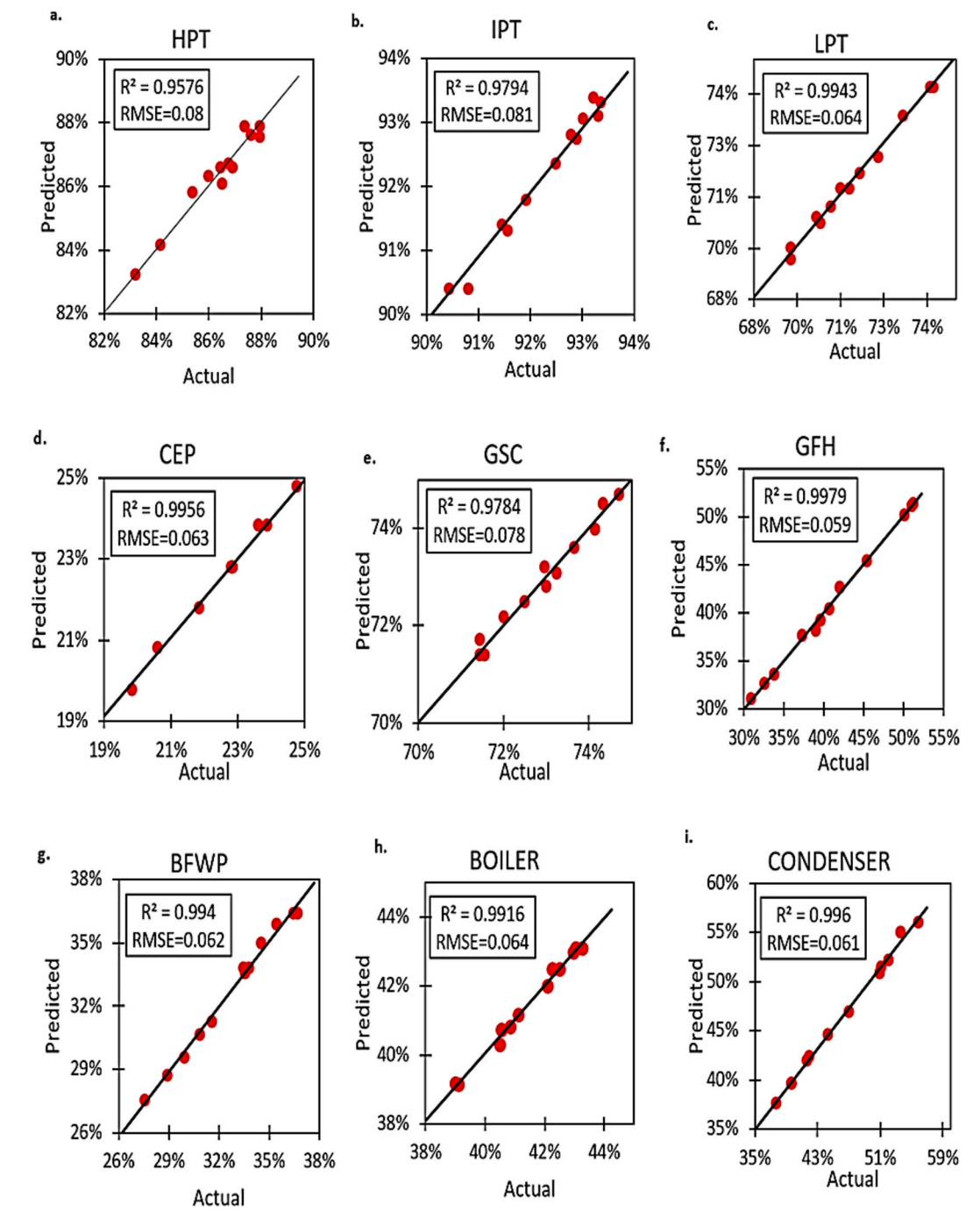


Fig. 10. Model performance for exergy efficiency at different stages of the plant: (a) HPT, (b) IPT, (c) LPT, (d) CEP, (e) GSC, (f) GFH, (g) BFWP, (h) Boiler, (i) Condenser.

improved by increasing their heat transfer surface area and sealing to prevent pressure drop, fluid leakage, and exergy loss.

• In this study, energy and exergy are set as a base for the performance evaluation of thermal systems. Although locations and magnitudes of energy losses have been described in detail, there is still a need to extend the analysis based on economic factors. Exergy analysis can be combined with economics to carry out exergy-economic analysis of power plants. Based on exergy destruction, a better estimation of costs can be allocated to thermal systems. The Random Tree Regression model is employed to predict energy efficiency and exergy efficiency within the power plant. The dataset is divided into training and testing data, utilizing a 70:30 ratio. The training data is instrumental in constructing and fine-tuning the model, while the

test data facilitates prediction generation. Comparing the predicted results with experimental data, the Root Mean Square Error (RMSE) is computed to assess model performance. Impressively, the overall average RMSE for energy efficiency is found to be 0.0852, and for exergy efficiency percentage, it is 0.068. These consistently low RMSE values validate the model's accuracy. The coefficient of determination (R2) for various stages of the power plant is computed by comparing the predicted results with experimental data. Notably, the overall average R2 value for energy analysis is 0.869, while for exergy analysis, it is 0.987. In addition, the study highlights the model's potential for optimizing power plant output parameters, providing valuable insights for future improvements. Expanding the dataset in subsequent research endeavors can further enhance the

model's precision. Moreover, the model's versatility enables evaluations across a wide range of values, contributing to the optimization of various facets of power plant performance.

- The current study applies AI models for the comprehensive analysis of power plants, particularly evaluating energy and exergy efficiency across different operational stages. While traditional thermodynamic modeling has been extensively used, integrating machine learning techniques such as Random Forest Regression modeling offers a more data-driven and adaptive method for predicting energy efficiency. Random Forest Regression modeling remains relatively underexplored in power plant analysis compared to conventional statistical approaches and other AI models like Support Vector Machines (SVM). However, it presents several advantages, making it a superior choice. Unlike SVM, which can struggle with large datasets and highdimensional feature spaces due to its computational complexity and sensitivity to hyperparameter tuning, Random Forest Regression modeling is inherently robust to overfitting and can handle complex relationships effectively. It is an ensemble learning approach that aggregates multiple decision trees and enhances predictive accuracy and generalizability, making it well-suited for complex, multi-stage power plant systems. By leveraging Random Forest Regression modeling for energy and exergy efficiency predictions, this study introduces a framework that improves accuracy, reduces computational overhead, and enhances decision-making for optimizing power plant performance.
- In addition, this research primarily focuses on the thermal aspects of the power plant—specifically, heat and energy losses in key components such as the boiler, turbine, and condenser—rather than the electrical generation process. However, by pinpointing components with maximum efficiency potential and those operating at lower efficiency, this study offers valuable insights for plant management to implement targeted improvements, minimize energy losses, and ultimately enhance electrical power generation.

4.1. Future outlook

Although the Random Forest Regression Model provides reliable predictions regarding energy and exergy analysis, in the future, the advanced machine learning models should be integrated with real-time power plant data for better optimization. The integration of advanced machine learning techniques offers significant potential for improving the accuracy and robustness of energy and exergy efficiency predictions. While Random Forest Regression has demonstrated reliability, future studies can explore deep learning models such as Artificial Neural Networks (ANN) and Long Short-Term Memory (LSTM) networks. These models can effectively capture complex nonlinear dependencies and enhance predictive capabilities. Furthermore, hybrid approaches combining machine learning with optimization techniques, such as Genetic Algorithms (GA) or Particle Swarm Optimization (PSO), could facilitate the determination of optimal operating conditions, leading to minimized exergy losses and enhanced plant efficiency. The implementation of real-time monitoring through digital twin technology and machine learning-driven predictive maintenance could further optimize operations, ensuring early anomaly detection and continuous performance improvements.

Expanding research to incorporate renewable energy sources, such as solar thermal and biomass, into the Rankine cycle could improve sustainability while reducing overall exergy destruction. Additionally, exploring supercritical and ultra-supercritical steam cycles may provide insights into their superior energy and exergy performance compared to conventional systems. Exergy-based economic and environmental assessments could further refine sustainability evaluations by considering carbon footprint reduction, cost-effectiveness, and lifecycle impacts. The effect of developing technologies, such as advanced thermal energy storage systems and supercritical CO₂ cycles, should be investigated to

improve the sustainability of large-scale power generation. The energy-exergy analysis could also be extended to explore the impact on the economic feasibility of power plants along with electricity production optimization. An exergy-economic viability assessment of intended efficiency improvements can help in decision-making for policymakers and operators of power plants. AI-driven fault diagnostics and dynamic exergy analysis under varying load conditions could enhance operational efficiency and reliability. Investigating advanced waste heat recovery technologies, such as Organic Rankine Cycles (ORC) or Kalina cycles, could further optimize rejected heat utilization. Lastly, benchmarking energy and exergy performance across different power plants would help establish industry-wide best practices and design improvements. Addressing these research directions will contribute to the advancement of intelligent energy management and sustainable power plant operations.

CRediT authorship contribution statement

Muhammad Ali Ijaz Malik: Writing – review & editing, Writing – original draft, Visualization, Software, Methodology, Investigation, Formal analysis, Data curation, Conceptualization. Adeel Ikram: Writing – review & editing, Writing – original draft, Visualization, Supervision, Software, Resources, Project administration, Methodology, Investigation, Funding acquisition, Formal analysis, Conceptualization. Sadaf Zeeshan: Writing – review & editing, Visualization, Software. Muhammad Naqvi: Writing – review & editing, Investigation. Syed Qasim Raza Zahidi: Investigation, Formal analysis. Fayaz Hussain: Writing – review & editing, Resources. Hayati Yassin: Writing – review & editing, Resources. Atika Qazi: Writing – review & editing.

Declaration of competing interest

The authors declare that they have no known competing financial interests or personal relationships that could have appeared to influence the work reported in this paper.

Acknowledgement

The authors sincerely acknowledge Superior University, Lahore, Pakistan, and the management of Balloki Power Plant, District Kasur, Punjab, Pakistan, for their invaluable support in facilitating data acquisition and ensuring the successful execution of the project. This industrial project was conceptualized and conducted under the supervision of Assistant Professor/Principal Investigator (PI), Dr. Adeel Ikram (Smart Manufacturing and Renewable Technologies Laboratory (SMART-Lab), Department of Mechanical Engineering, Superior University, Lahore, Pakistan) and coordinated by co-PI, Mr. Muhammad Ali Ijaz Malik, a member of the Industrial Liaison Committee/Lecturer in the Department of Mechanical Engineering, Superior University Lahore, Pakistan.

Data availability

Data will be made available on request.

References

- Naeimi J, Biglari M, Zirak S, Jafari Gavzan I. Enhancing conventional steam power plant performance through feed water heating repowering. Energy Sources Part A 2024;46(1):18–34.
- [2] Salman CA, Naqvi M, Thorin E, Yan J. Impact of retrofitting existing combined heat and power plant with polygeneration of biomethane: A comparative technoeconomic analysis of integrating different gasifiers. Energ Conver Manage 2017; 152:250-65.
- [3] Erdem HH, et al. Comparative energetic and exergetic performance analyses for coal-fired thermal power plants in Turkey. Int J Therm Sci 2009;48(11):2179–86.

- [4] Valasai GD, Uqaili MA, Memon HR, Samoo SR, Mirjat NH, Harijan K. Overcoming electricity crisis in Pakistan: A review of sustainable electricity options. Renew Sustain Energy Rev 2017;72:734-45.
- Kessides IN. Chaos in power: Pakistan's electricity crisis. Energy Policy 2013;55:
- [6] Khan MA, Ali A, Zakaria M. Analysis of power plants in China Pakistan economic corridor (CPEC): An application of analytic network process (ANP). J Renew Sustain Energy, vol. 10, no. 6, 2018.
- [7] N. g. world. "PAKISTAN'S LNG OPTIONS [GAS IN TRANSITION]." https://www. naturalgasworld.com/pakistans-lng-options-gas-in-transition-95542 (accessed.
- (2022). Energy. [Online] Available: https://www.finance.gov.pk/survey/ chapter_22/PES14-ENERGY.pdf.
- N. g. world. "HOW CAN NATURAL GAS HELP PAKISTAN EMERGE STRONGER FROM PAST DIFFICULTIES?" https://www.naturalgasworld.com/early-releasehow-can-natural-gas-help-pakistan-emerge-stronger-from-past-difficulties-ggp-106933#:~:text=Pakistan's%20LNG%20import%20capacity%20is,expected% 20to%20come%20online%20soon. (accessed.
- [10] Elwardany M, Nassib A, Mohamed HA, Abdelaal M. Energy and exergy assessment of 750 MW combined cycle power plant: A case study. Energy Nexus
- [11] Huang G, Huang C, Liu H, Huang H, Shang W, Wang W. Exergy analysis of offdesign performance in solar-aided power generation systems: Evaluating the rationality of using part-load operation solution of coal-fired plants. Energy 2024:
- [12] Utlu Z, Hepbasli A. A review on analyzing and evaluating the energy utilization efficiency of countries. Renew Sustain Energy Rev 2007;11(1):1-29.
- [13] Pattanayak L, Sahu JN, Mohanty P. Combined cycle power plant performance evaluation using exergy and energy analysis. Environ Prog Sustain Energy 2017; 36(4):1180-6.
- [14] Kaya AM, Kandemir İ, Akşit MF, Yiğit KS. Investigation of optimum working conditions of a micro cross flow turbine. Environ Prog Sustain Energy 2015;34(5): 1506-11.
- [15] Elhelw M, Al Dahma KS. Utilizing exergy analysis in studying the performance of steam power plant at two different operation mode. Appl Therm Eng 2019;150:
- [16] Aliyu M, AlQudaihi AB, Said SA, Habib MA. Energy, exergy and parametric analysis of a combined cycle power plant. Therm Sci Eng Prog 2020;15:100450.
- [17] Kaska Ö. Energy and exergy analysis of an organic Rankine for power generation from waste heat recovery in steel industry. Energ Conver Manage 2014:77: 108-17.
- Aljundi IH. Energy and exergy analysis of a steam power plant in Jordan. Appl Therm Eng 2009;29(2–3):324–8.
- [19] Amir V. Improving steam power plant efficiency through exergy analysis: ambient temperature. In: 2nd international Conference on Mechanical. Production and Automobile Engineering (ICMPAE) Singapore, 2012: Citeseer, pp.
- Regulagadda P, Dincer I, Naterer G. Exergy analysis of a thermal power plant with measured boiler and turbine losses. Appl Therm Eng 2010;30(8-9):970-6.
- Kaushik S, Reddy VS, Tyagi S. Energy and exergy analyses of thermal power
- plants: A review. Renew Sustain Energy Rev 2011;15(4):1857–72. Ameri M, Ahmadi P, Khanmohammadi S. Exergy analysis of a 420 MW combined cycle power plant. Int J Energy Res 2008;32(2):175-83.
- Ameri M, Ahmadi P, Hamidi A. Energy, exergy and exergoeconomic analysis of a steam power plant: A case study. Int J Energy Res 2009;33(5):499-512.
- **[24]** Ahmadi GR, Toghraie D. Energy and exergy analysis of Montazeri steam power plant in Iran. Renew Sustain Energy Rev 2016;56:454–63.
- [251 Rudiyanto B. et al., Energy and Exergy Analysis of steam power plant in Paiton, Indonesia. In: IOP Conference Series: Earth and Environmental Science, 2019, vol. 268, no. 1: IOP Publishing, p. 012091.
- **[26]** Pilankar KD, Kale R. Energy and exergy analysis of steam and power generation plant. Int J Eng Techn Res 2016;5:344-50.
- Danish MSS, Nazari Z, Senjyu T. AI-coherent data-driven forecasting model for a [27] combined cycle power plant. Energ Conver Manage 2023;286:117063.
- Assareh E, Firoozzadeh M, Zoghi M, Zare A, Ghazi Y, Shahin-Banna A. Water desalination using waste heat recovery of thermal power plant in tropical climate; optimization by AI. Energy Convers Manage: X 2024;24:100731.
- Beiron J, Göransson L, Normann F, Johnsson F. Flexibility provision by combined heat and power plants-An evaluation of benefits from a plant and system perspective. Energy Convers Manage: X 2022;16:100318.
- [30] Moghaddam AH, Esfandyari M, Jafari D, Sakhaeinia H. Multi-factor optimization of bio-methanol production through gasification process via statistical methodology coupled with genetic algorithm. Results Eng 2023;20:101477.
- [31] Jair C, Farid G-L, Lisbeth R-M, Asdrubal L. A comprehensive survey on support vector machine classification: Applications, challenges and trends. Neurocomputing 2020;408:189-215.
- Akshit K, Pavan D, Aarya V, Manan S. A Comprehensive Comparative Study of Artificial Neural Network (ANN) and Support Vector Machines (SVM) on Stock Forecasting. Ann Data Sci 2023;10.
- [33] Mehdi H, Amir Masoud R, Bay V, Moazam B, Mohammad M, Mehran Z. Improving security using SVM-based anomaly detection: issues and challenges. Soft Comput 2021;25:3195-223.
- Vinod Kumar C, Kalpana D, Anuj S. Problem formulations and solvers in linear SVM: a review. Artif Intell Rev 2019;52:803-55.
- Maher MGM, et al. Artificial neural networks based optimization techniques: a review. Electronics 2021;10(21):2689.

- [36] Oludare Isaac A, Aman J, Abiodun Esther O, Kemi Victoria D, Abubakar Malah U, Okafor Uchenwa L. Comprehensive Review of Artificial Neural Network Applications to Pattern Recognition. IEEE Access 2019;7:158820-46.
- Mahdi S, Alexandra S-L, Nilay S. Machine-learning methods for integrated renewable power generation: A comparative study of artificial neural networks, support vector regression, and Gaussian Process Regression. Renew Sustain Energy Rev 2019;108:513–38.
- [38] Konstantinov AV, Utkin LV. Interpretable machine learning with an ensemble of gradient boosting machines. Knowl-Based Syst 2021;222:106993
- Manoharan A, Begam KM, Aparow VR, Sooriamoorthy D. Artificial Neural Networks, Gradient Boosting and Support Vector Machines for electric vehicle battery state estimation: A review. J Storage Mater 2022;55:105384.
- Timur B, Johannes J. Oil Production Monitoring using Gradient Boosting Machine Learning Algorithm. IFAC-PapersOnLine 2019;52:514-9.
- Speiser JL, Miller ME, Tooze J, Ip E. A comparison of random forest variable selection methods for classification prediction modeling. Expert Syst Appl 2019; 134:93-101.
- [42] Yile A, Hongqi L, Liping Z, Sikandar A, Zhongguo Y. The linear random forest algorithm and its advantages in machine learning assisted logging regression modeling. J Pet Sci Eng 2019;174:776-89.
- [43] Zhigang S, Guotao W, Pengfei L, Hui W, Min Z, Xiaowen L. An improved random forest based on the classification accuracy and correlation measurement of decision trees. Expert Syst Appl 2024;237:121549.
- Shanmugasundar G, Vanitha M, Čep R, Kumar V, Kalita K, Ramachandran M. A comparative study of linear, random forest and adaboost regressions for modeling non-traditional machining. Processes 2021;9(11):2015.
- [45] H. Mariana, M. Omar, E. Wejdan Abu, and M. Mustafa, "Performance prediction of a clean coal power plant via machine learning and deep learning techniques," Energy & Environment, vol. 35, 2024.
- Min Kyeong P, Jong Man L, Won He K, Jong Min C, Kwang Ho L. Predictive model for PV power generation using RNN (LSTM). J Mech Sci Technol 2021;35: 795–803.
- [47] Moustafa EB, Hammad AH, Elsheikh AH. A new optimized artificial neural network model to predict thermal efficiency and water yield of tubular solar still. Case Stud Therm Eng 2022;30:101750.
- Morteza E, Amin Amiri D, Ali J. Optimization of ultrasonic-excited double-pipe heat exchanger with machine learning and PSO. Int Commun Heat Mass Transfer 2023;147:106985.
- A. Ehsanolah, F. M. Mohammad, Zoghi, Z. Ali, G. Yasaman, and S.-B. Ali, "Water desalination using waste heat recovery of thermal power plant in tropical climate; optimization by AI," Energy Conversion and Management: X, vol. 24, p. 100731, 2024.
- [50] Mojtaba E, Dariush J. Prediction of thiophene removal from diesel using [BMIM] [AlCl4] in EDS Process: GA-ANFIS and PSO-ANFIS modeling. Pet Sci Technol 2018:36(16):1305-11.
- [51] Xuerong C, Rong-Jong W. Intelligent DC Arc-Fault Detection of Solar PV Power Generation System via Optimized VMD-Based Signal Processing and PSO-SVM. IEEE J Photovoltaics 2022;12(4):1058-77.
- Waqar Muhammad A, et al. Artificial intelligence enabled efficient power generation and emissions reduction underpinning net-zero goal from the coalbased power plants. Energ Conver Manage 2022;268:116025.
- Guo-Qian L, Ling-Ling L, Ming-Lang T, Han-Min L, Dong-Dong Y, T. Raymond R. An improved moth-flame optimization algorithm for support vector machine prediction of photovoltaic power generation. J Clean Prod 2020;253:119966.
- Wumaier T, Xu C, Guo H, Jin Z, Zhou H, Fault Diagnosis of Wind Turbines Based on a Support Vector Machine Optimized by the Sparrow Search Algorithm. IEEE Access 2021:9:69307-15.
- [55] Upma S, Mohammad R, Muhannad A, Ibrahim A. A Machine Learning-Based Gradient Boosting Regression Approach for Wind Power Production Forecasting: A Step towards Smart Grid Environments. Energies 2021;14:5196.
- Georgios M, Hendrik L. An interpretable probabilistic model for short-term solar power forecasting using natural gradient boosting. Appl Energy 2022;309: 118473
- [57] Chenhao H, et al. AI-based carbon peak prediction and energy transition optimization for thermal power industry in energy-intensive regions of China. Energ Conver Manage 2025:X:100884.
- A. Edianto, G. Trencher, N. Manych, and K. Matsubae, "Forecasting coal power plant retirement ages and lock-in with random forest regression," Patterns, 2023.
- A. Khalyasmaa et al., "Prediction of solar power generation based on random forest regressor model," in 2019 International Multi-Conference on Engineering, Computer and Information Sciences (SIBIRCON), 2019: IEEE, pp. 0780-0785.
- Babar B, Luppino LT, Boström T, Anfinsen SN. Random forest regression for improved mapping of solar irradiance at high latitudes. Sol Energy 2020;198: 81_92
- Villegas-Mier CG, Rodriguez-Resendiz J, Álvarez-Alvarado JM, Jiménez-Hernández H, Odry Á. Optimized random forest for solar radiation prediction using sunshine hours. Micromachines 2022;13(9):1406.
- Singh U, Rizwan M, Alaraj M, Alsaidan I. A machine learning-based gradient boosting regression approach for wind power production forecasting: A step towards smart grid environments. Energies 2021;14(16):5196.
- Lee J, Wang W, Harrou F, Sun Y. Wind power prediction using ensemble learningbased models. IEEE Access 2020;8:61517-27.
- Arrieta-Prieto M, Schell KR. Spatially transferable machine learning wind power prediction models: v- logit random forests. Renew Energy 2024;223:120066.

- [65] Jonkers J, Avendano DN, Van Wallendael G, Van Hoecke S. A novel day-ahead regional and probabilistic wind power forecasting framework using deep CNNs and conformalized regression forests. Appl Energy 2024;361:122900.
- [66] Iannace G, Ciaburro G, Trematerra A. Wind turbine noise prediction using random forest regression. Machines 2019;7(4):69.
- [67] Ahmed MM, Robin HM, Shahadat MMZ, Masud MH. Innovative approaches for reducing wind turbine noise: A review from mechanical and aerodynamic perspective. Energy Rep 2025;13:728-46.
- Yang H, Yuan W, Zhu W, Sun Z, Zhang Y, Zhou Y. Wind turbine airfoil noise prediction using dedicated airfoil database and deep learning technology. Appl Energy 2024;364:123165.
- Kwak S, et al. Machine learning prediction of the mechanical properties of γ -TiAl alloys produced using random forest regression model. J Mater Res Technol 2022;
- Li H, Lin J, Lei X, Wei T. Compressive strength prediction of basalt fiber reinforced concrete via random forest algorithm. Mater Today Commun 2022;30:
- [71] Ricardo F, Ruiz-Puentes P, Reyes LH, Cruz JC, Alvarez O, Pradilla D. Estimation and prediction of the air-water interfacial tension in conventional and peptide surface-active agents by random Forest regression. Chem Eng Sci 2023;265:
- [72] Kishino M, Matsumoto K, Kobayashi Y, Taguchi R, Akamatsu N, Shishido A. Fatigue life prediction of bending polymer films using random forest. Int J Fatigue 2023:166:107230.
- Palomino AF, Espino PS, Reyes CB, Rojas JAJ, y Silva FR. Estimation of moisture in live fuels in the mediterranean: Linear regressions and random forests. J Environ Manage 2022;322:116069.
- [74] Morris JD, Daood SS, Nimmo W. Machine learning prediction and analysis of commercial wood fuel blends used in a typical biomass power station. Fuel 2022;
- Chen ZS, Lam JSL, Xiao Z. Prediction of harbour vessel fuel consumption based on machine learning approach. Ocean Eng 2023;278:114483.
- Turja AI, Sadat KN, Hasan MM, Khan Y, Ehsan MM. Waste Heat Recuperation in Advanced Supercritical CO2 Power Cycles with Organic Rankine Cycle Integration & Optimization Using Machine Learning Methods. Int J Thermofluids 2024:22:100612
- [77] A. B. A. Mansur Aliyu, Syed A.M. Said*, Mohamed A. Habib, Energy, exergy and parametric analysis of a combined cycle power plant, Therm Sci Eng Progr, vol. 15, 2020.
- [78] Gholam Reza Ahmadi DT. Energy and exergy analysis of Montazeri Steam Power
- Plant in Iran. Therm Sci Eng Prog 2016;56:454-63.
 [79] Erdem HH, Akkaya AV, Cetin B, Dagdas A, Sevilgen SH, Sahin B, et al. Comparative energetic and exergetic performance analyses for coal-fired thermal power plants in Turkey. Int J Therm Sci 2009;48:2179-86.
- Pattanayak JNSL, Mohantye P. Combined Cycle Power Plant Performance [80] Evaluation Using Exergy and Energy Analysis. Environ Prog Sustain Energy 2017.
- Regulagadda IDP, Naterer GF. Exergy analysis of a thermal power plant with measured boiler and turbine losses. Appl Therm Eng 2010;30:970-6.
- Ganapathy T, Alagumurthi N, Gakkhar RP, Murugesan K. Exergy analysis of operating lignite fired thermal power plant. J Eng Sci Technol Rev 2009:123–30.
- Aljundi IH. Energy and exergy analysis of a steam power plant in Jordan. Appl Therm Eng 2009;29:324-8.
- Li X, Gao J, Zhang Y, Zhang Y, Du Q, Wu S, et al. Energy, Exergy and Economic Analyses of a Combined Heating and Power System with Turbine-Driving Fans and Pumps in Northeast China, Energies 2020.
- Kaska Ö. Energy and exergy analysis of an organic Rankine for power generation from waste heat recovery in steel industry. Energ Conver Manage 2014;77: 108-17

- [86] F. B. Thamir K. Ibrahim, Omar I. Awad, Ahmed N. Abdullah, G. Najafi, Rizlman Mamat, F.Y. Hagos. (2017). Thermal performance of gas turbine power plant based on exergy analysis.
- Babaei Jamnani AKM. Energy-exergy performance assessment with optimization guidance for the components of the 396-MW combined-cycle power plant. Energy Sci Eng 2020.
- Mitrovic DZD, Lakovic MS. Energy and Exergy Analysis of a 348.5 MW Steam Power Plant. Energy Source 2010;32:1016–27.
- Rudiyanto B, Wardani TA, Anwar S, Al Jamali L, Prasetyo T, Wibowo KM, et al. Energy and Exergy Analysis of Steam Power Plant in Paiton, Indonesia. Int Conf Sustain Energy Green Technol 2018.
- Pilankar KD, Kale R. Energy and Exergy Analysis of Steam and Power Generation Plant. Int J Eng Res Technol, vol. 5, no. 6, 2016.
- Mehrabi Gohari E, Pishkar I, Omidian E. Energy and exergy analysis of steam power plant cycle of the ninth refinery of south pars gas complex. Iranica J Energy Environ 2025:124–35.
- [92] Vivek Kumar VKS, Kumar R, Kumar Shravan. Energy, exergy, sustainability and environmental emission analysis of coal-fired thermal power plant. Ain Shams Eng J 2024.
- [93] Elwardany M, Nassib AM, Mohamed HA. Exergy analysis of a gas turbine cycle power plant: a case study of power plant in Egypt. J Therm Anal Calorim 2024.
- Ahmadi GR, Toghraie D. Energy and exergy analysis of Montazeri Steam Power Plant in Iran. Renew Sustain Energy Rev 2016:454-63.
- Moran MJ, Shapiro HN, Boettner DD, Bailey MB. Fundamentals of engineering thermodynamics. John Wiley & Sons; 2010.
- Bimestre TA, Júnior JAM, Canettieri EV, Tuna CE, Sobrinho PM. Energy Efficiency Technologies for Hydroelectric Power Plants: A Case Study in Brazil. J Power Energy Eng 2022;10(5):90–115.
- Yang Y, et al. Life cycle assessment of typical tower solar thermal power station in China. Energy 2024;309:133154.
- Vundela Siva R, Subash Chndra K, Sudhir Kumar T, Narayanlal P. An approach to analyse energy and exergy analysis of thermal power plants: a review. Smart Grid Renewa Energy 2010;2010.
- [99] Bari SA, Fuad M, Labib KF, Ehsan MM, Khan Y, Hasan MM. Enhancement of thermal power plant performance through solar-assisted feed water heaters: An innovative repowering approach. Energy Convers Manage: X 2024;22:100550.
- [100] Li X, et al. Energy, exergy and economic analyses of a combined heating and power system with turbine-driving fans and pumps in Northeast China. Energies 2020;13(4):878.
- [101] Calise F, Palombo A, Vanoli L. Design and partial load exergy analysis of hybrid SOFC-GT power plant. J Power Sources 2006;158(1):225-44.
- Gümüş M, Atmaca M. Energy and exergy analyses applied to a CI engine fueled with diesel and natural gas. Energy Sources Part A 2013;35(11):1017–27.
- Babaei Jamnani M, Kardgar A. Energy-exergy performance assessment with optimization guidance for the components of the 396-MW combined-cycle power plant. Energy Sci Eng 2020;8(10):3561–74.
- [104] Dincer I, Al-Muslim H. Thermodynamic analysis of reheat cycle steam power plants. Int J Energy Res 2001;25(8):727-39.
- Ahmadi GR, Toghraie D. Energy and Exergy Analysis of Montazeri Steam Power Plant in Iran, Renew Sustain Energy Rev 2016;56:454-63.
- [106] Rashad A, El Maihy A. Energy and exergy analysis of a steam power plant in Egypt. In: In 13th International Conference on Aerospace Sciences & Aviation
- Technology; 2009. p. 1–12.

 [107] Sanjay Y, Singh O, Prasad B. Energy and exergy analysis of steam cooled reheat gas-steam combined cycle. Appl Therm Eng 2007;27(17-18):2779-90.